Molecular Therapy
Methods & Clinical Development
Original Article

Comparison of highly pure rAAV9 vector stocks produced in suspension by PEI transfection or HSV infection reveals striking quantitative and qualitative differences

Prasad D. Trivedi,[1] Chenghui Yu,[1,2] Payel Chaudhuri,[1] Evan J. Johnson,[1] Tina Caton,[1] Laura Adamson,[1] Barry J. Byrne,[1] Nicole K. Paulk,[3] and Nathalie Clément[1]

[1]Department of Pediatrics, Powell Gene Therapy Center, University of Florida, Gainesville, FL 32610, USA; [2]State Key Laboratory of Genetic Engineering, School of Life Sciences, Fudan University, Shanghai 200438, China; [3]Department of Biochemistry & Biophysics, University of California San Francisco, San Francisco, CA 94158, USA

Recent clinical successes have propelled recombinant adeno-associated virus vectors (rAAV) to the center stage for human gene therapy applications. However, the exploding demand for high titers of highly pure rAAV vectors for clinical applications and market needs remains hindered by challenges met at the manufacturing stage. The production of rAAV by transfection in suspension cells remains one of the most commonly used production platforms. In this study, we describe our optimized protocol to produce rAAV by polyethyleneimine (PEI)-mediated transfection in suspension HEK293 cells, along with a side-by-side comparison to our high-performing system using the herpes simplex virus (HSV). Further, we detail a new, robust, and highly efficient downstream purification protocol compatible with both transfection and infection-based harvests that generated rAAV9 stocks of high purity. Our in-depth comparison revealed quantitative, qualitative, and biological differences between PEI-mediated transfection and HSV infection. The HSV production system yielded to higher rAAV vector titers, higher specific yields, and a higher percentage of full capsids than transfection. Furthermore, HSV-produced stocks had a significantly lower concentration of residual host cell proteins and helper DNA impurities, but contained detectable levels of HSV DNA. Importantly, the potency of PEI-produced and HSV-produced rAAV stocks were identical. Analyses of AAV Rep and Cap expression levels and replication showed that HSV-mediated production led to a lower expression of Rep and Cap, but increased levels of AAV genome replication. Our methodology enables high-yield, high purity rAAV production and a biological framework to improve transfection quality and yields by mimicking HSV-induced biological outcomes.

INTRODUCTION

Recent clinical successes, along with three recently marketed products[1] have propelled recombinant adeno-virus viral vectors (rAAV) to the center stage for human gene therapy applications. However, the exploding demand for highly pure and high titer rAAV vectors for clinical and market needs remains hindered by challenges met at the manufacturing stage. The lack of high-performing and robust production systems often results in delays or failure to meet the target yield or quality required by the U.S. Food and Drug Administration (FDA). Innovative improvements and the establishment of robust and scalable processes have become a priority undertaking in the field.[2]

Wild-type adeno-associated virus (wtAAV) is a parvovirus member of the dependovirus subgroup owing to its dependence on a helper virus, such adenovirus or herpesvirus, to replicate and produce progeny virions in permissive cells. The virus is composed of a short 4.7-Kb single-stranded DNA genome with two hairpin-shaped inverted terminal repeats (ITRs) at each end, packaged into an icosahedral protein capsid of about 26 nM in diameter. The recombinant AAV genome only retains the ITRs from wtAAV serotype 2 (AAV-2), which act as a viral original of replication and are required for rescue, replication and packaging of the recombinant genome.[3,4] The wtAAV genome has two predominant, in-frame, open reading frames, Rep and Cap. Rep codes for four Rep proteins (Rep 78, 68, 52, and 40), which are essential for the genome rescue, replication, and encapsidation, among others functions, and precisely regulate AAV gene expression during the virus' life cycle. Cap codes for three capsid proteins (VP1, 2, and 3) that form the capsid.[3,5,6] Two other non-structural proteins, from an out-of-frame open reading frame (ORF) within Cap, the assembly-activating protein[7] and the membrane-associated accessory protein[8] have been associated with packaging functions. During the wild-type virus replication cycle, the tightly controlled levels of AAV gene expression are keys to supporting

Received 14 August 2021; accepted 22 December 2021;
https://doi.org/10.1016/j.omtm.2021.12.006.

Correspondence: Nathalie Clément, Ph.D, Department of Pediatrics, Powell Gene Therapy Center, University of Florida, 1200 Newell Drive, Academic Research Building, RG-187, Gainesville, FL 32610, USA.
E-mail: nclement@peds.ufl.edu

optimal virus assembly. Failure to recreate the kinetics and level of expression of these non-structure and structural proteins often leads to low-performing or poor-quality production platforms. In permissive cells, wtAAV gene expression is also controlled by cellular genes and helper genes provided by the helper virus, which are, in turn, controlled by various metabolic phases of the host cell.[5,9,10] Standard rAAV production protocols recapitulate this virus replication cycle by providing both Rep and Cap expression sequences and the helper virus functions, *in trans*, using either a plasmid DNA (transfection methods with Ad5 functions)[4,11,12] or a recombinant helper virus genome such HSV-1 or baculovirus (infection-based methods).[13,14] Both for transfection or infection-mediated production, the gene of interest (GOI) is provided by a plasmid or recombinant virus that carries the expression cassette flanked by AAV-2 ITRs. Production is triggered by providing AAV-GOI, AAV-Rep/Cap, and helper virus functions in the host cell by transfection or infection.

To date, the field has not adopted a unified production method or downstream process; rather, each group implements their own to meet their needs with regard to serotype diversity, clinical yields, or intellectual property requirements.[2] However, transfection in suspension using polyethyleneimine (PEI) has become the most commonly used production method in recent years,[15,16] because of its many favorable features: simple implementation, availability and low cost of the raw materials, and flexibility to be used with many different genomic constructs. This is in sharp contrast with systems based on Baculovirus,[14] stable producer cell lines,[17–19] or HSV,[2,20,21] all of which require time-consuming preparation of raw materials before production. Additionally, the PEI method benefits from the long-standing clinical safety profile from the use of the traditional calcium phosphate-based transfection methods to produce rAAV over the past two decades.[2,3]

In our previous work, we demonstrated the superiority of the HSV method when used in suspension in HEK293 cells with respect to rAAV titers and quality.[21–23] In the current work, we developed a PEI-based production method for rAAV in a suspension-based format using the same commercial Expi293F cell line used successfully with our HSV platform. The current study presents a detailed side-by-side comparison of a PEI transfection and an HSV infection platform in suspension. First, we describe two optimized PEI-based production protocols in suspension HEK293 cells, as well as a novel downstream protocol to support the purification of both PEI- and HSV-produced rAAV9. Our analytical comparison study assessed vector yields and qualitative characteristics, including vector potency, ratio of full-to-empty capsids, residual host cell proteins (HCP) and residual helper DNA, capsid post-translational modifications. Last, the expression kinetics and levels of AAV rep and cap genes and the vector genome replication were also assessed.

RESULTS

Optimization of PEI transfection for AAV production

Numerous protocols describing the production of rAAV vectors by PEI transfection are available. However, in light of the variety of materials and reagents available, cell culture media, HEK293 derivatives, cell culture vessels, and equipment, we evaluated and optimized the method in our laboratory. We built our strategy based on our expertise working with Expi293F cells in disposable shaker flasks for HSV-mediated production.[22] To support a direct comparison, we aimed to maintain the parameters between HSV- and PEI-mediated production as similar as possible. In addition, our protocol used a two-plasmid transfection protocol, rather than the widely used triple transfection one, in which a single helper plasmid, pDG-UF9-KanR, carries both AAV2 Rep and AAV9 Cap sequences and the Ad5 helper functions.[21,24] Vector production is initiated by co-transfecting the AAV plasmid, pTRUF5, that contains AAV2 ITRs and a cytomegalovirus-green fluorescent protein (CMV-GFP) expression cassette, with this single helper. Importantly, our two-plasmid transfection design closely mimics the HSV co-infection-based production protocol, where one recombinant HSV (rHSV) carries the exact same rAAV genome as the one present in pTRUF5, and one rHSV carries the AAV2 Rep/AAV9 Cap cassette.

In this work, we assessed a series of parameters that included PEI-to-plasmid ratio, plasmid-to-plasmid ratio, total plasmid DNA amount, cell concentration, and PEI/DNA-to-cell ratio, as well as the timing of the production harvest. We also compared two different brands of PEI, PEI Max, a well-documented reagent for AAV production,[15,16] and the more recently launched PEI Prime.

PEI Max

In the first set of experiments, we concomitantly assessed three AAV-to-helper plasmid molar ratios, 1:1, 1:2, and 1:3, and three PEI-to-DNA ratios of 1:1, 2:1, and 3:1. The total amounts of DNA and cells were set to 50 μg and 5×10^7, respectively, in a 50-mL production volume. Vector genome (vg) titers were measured in each of the benzonase-treated cell harvests, collected 72 h after transfection (Figure 1A). Although not significantly different, we found that the best vg yield was obtained with a PEI Max-to-DNA ratio of 2:1 and a plasmid-to-plasmid ratio of 1:1, with about 2×10^{12} vg per flask. We maintained these parameters for the rest of the experiments. Next, we varied the cell concentration from 1×10^6 to 4×10^6 cell/mL in a 50-mL final volume and either kept the total DNA constant or increased proportionally to the cell concentration. We measured both vg titers and transducing unit (TU) titers for each condition (Figure S1A). We observed that increasing the cell density from 1 to 3×10^6 c/mL did not result in a significant vg increase, but 2×10^6 cells/mL yielded to a 50% increase, both in vg and TU titers, when compared with 1×10^6 cells/mL. Greater cell concentrations resulted in a yield decrease. We further adjusted the amount of plasmid, both at 1 or 2×10^6 cells/mL with intermediate DNA amounts and found that the optimal amount of DNA for a concentration of 1×10^6 cells/mL was 50 μg, and 75 μg for 2×10^6 cells/mL (Figure 1B). The three best conditions were repeated over a larger number of biological replicates and confirmed the optimal condition to be 2×10^6 cell/mL with 75 μg DNA (Figure 1C) ($p < 0.001$). The average yield with this condition was $6.24 \times 10^{12} \pm 4.90 \times 10^{12}$ vg, which would correspond with approximately 1×10^{14} vg/L and a specific yield of 6.24×10^4 vg/cell $\pm 4.9 \times 10^4$ ($n = 12$). The infectivity of

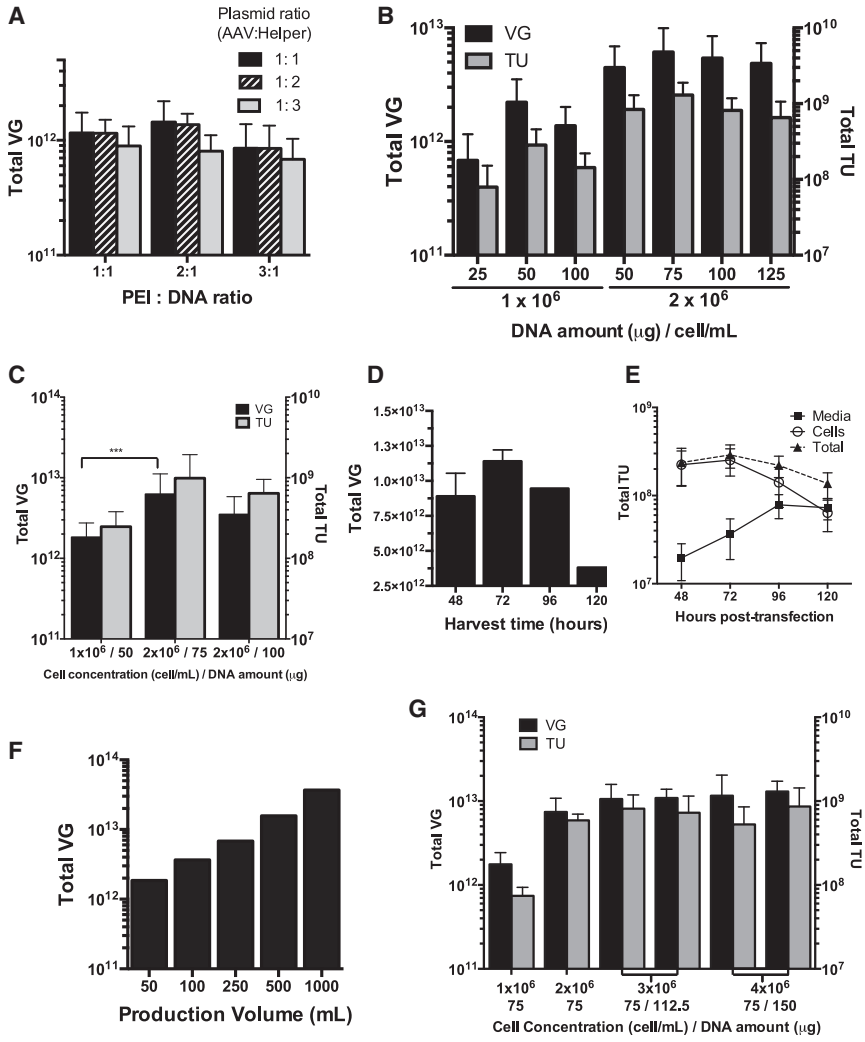

Figure 1. Parameter optimization for PEI-mediated transfection in suspension HEK293

(A) Plasmids and PEI Max ratios. We transfected 5×10^7 Expi293F cells with PEI Max, pTRUF5, and pDG-UF9-KanR (50 μg total DNA) in 50 mL final production volume in nine different conditions: pTRUF5-to-pDG-UF9-KanR molar ratio 1:1 (black bar), 1:2 (dashed bars), and 1:3 (gray bars); the PEI-to-DNA amount 1:1, 2:1, and 3:1 (x axis). Cell pellets were harvested 72 h after transfection, lysed, digested with benzonase, and submitted to real-time qPCR for vg titers. Averages and SD plotted, n = 4 independent experiments (biological replicates). (B) Cell density and total DNA amount for PEI Max. Cell concentrations of 1×10^6 and 2×10^6 cell/mL were prepared (50 mL, 5×10^7 and 1×10^8 cells). Various DNA amounts (x axis) were tested with the plasmid molar ratio at 1:1. Cell harvests were prepared as described in (A) and vg titers (black bars) and TU titers (gray bars) determined. Yield averages and SD (VG, left axis; TU, right axis) plotted, n = 4 independent experiments. (C) Statistical determination of optimal conditions for PEI Max. Transfections were repeated using the three best conditions identified and total yields measured for vgs (black bars) and TUs (gray bars). Averages and SD are shown for 1×10^6 cell/mL, 50 μg, n = 25; 2×10^6 cell/mL, 75 μg n = 12; and 2×10^6 cell/mL, 100 μg for n = 11 (n = biological replicates). $p \leq 0.001$. (D) Time of harvest. Cells (50 mL, 5×10^7 cells) were transfected (50 μg DNA) at time 0 in four separate flasks. Each flask was harvested at either 48, 72, 96, or 120 h after transfection and VG yields assessed. Average and SD plotted at 48 and 72 (n = 3 biological replicates) and 96 and 120 h (n = 1). (E) Viral particles distribution between cells and media over time. Transfections were performed in the same conditions described in (D), but cells and media were collected at each time point and evaluated for TUs. Averages and SD for three independent experiments. (F) Scale-up. Transfections were performed with same conditions as in (D), but with the volume increased from 50 mL to 1 L and amounts of DNA and PEI increased proportionally. Cell harvests were obtained after 72 h and analyzed for VG titer and yield (n = 1 representative experiment). (G) Parameters optimization for PEI Prime. The cell concentration was increased from 1×10^6 to 4×10^6 cell/mL (x axis) in a constant 50 mL culture volume (5×10^7 to 2×10^8 cells) and a PEI-to-DNA ratio of 3. Total plasmid DNA amount was set either constant at 75 μg or proportionally increased to the cell concentration (x axis legend). The average yields in vg titers and TUs and SD for n = 3 for 1×10^6 cell/mL and for n = 7 for 2 to 4×10^6 cell/mL.

the rAAV9 vector particles produced was similar across these three conditions as measured by the ratio of VG:TU (Figure S1B).

We next established that harvest at 2, 3, or 4 days after transfection resulted in relatively similar yields (Figure 1D), with a peak at 3 days after transfection. Harvests beyond 4 days resulted in a sharp vector yield decrease. When analyzing the rAAV9 vector infectious particles present in the cells versus the media, we noted that, at 3 days after transfection, the majority of the rAAV particles remained within the cells and only 10% were in the media. At 4 and 5 days after transfection, the percentage of AAV particles in the media significantly increased, up to 50% of the total (Figure 1E), but the total yield (cells plus media) did not exceed the yield obtained at 3 days. These results were in line with our calcium phosphate transfection protocol in adherent cells, as well as our co-infection protocol with rHSV in suspension cells.[22]

Scalability of the PEI transfection method

To generate enough material to undertake a thorough comparison study, as well as establish a novel purification process for rAAV9, we evaluated the scalability of the method from 50 mL to 1 L. The increase in rAAV particles produced in the cell harvests was linearly correlated with the production volumes tested and with a volumetric yield of approximately 3.40×10^{13} vg/L (Figure 1F).

PEI Prime

The optimization set forth for PEI Prime was built on the data obtained for PEI Max and only a subset of parameters was re-assessed,

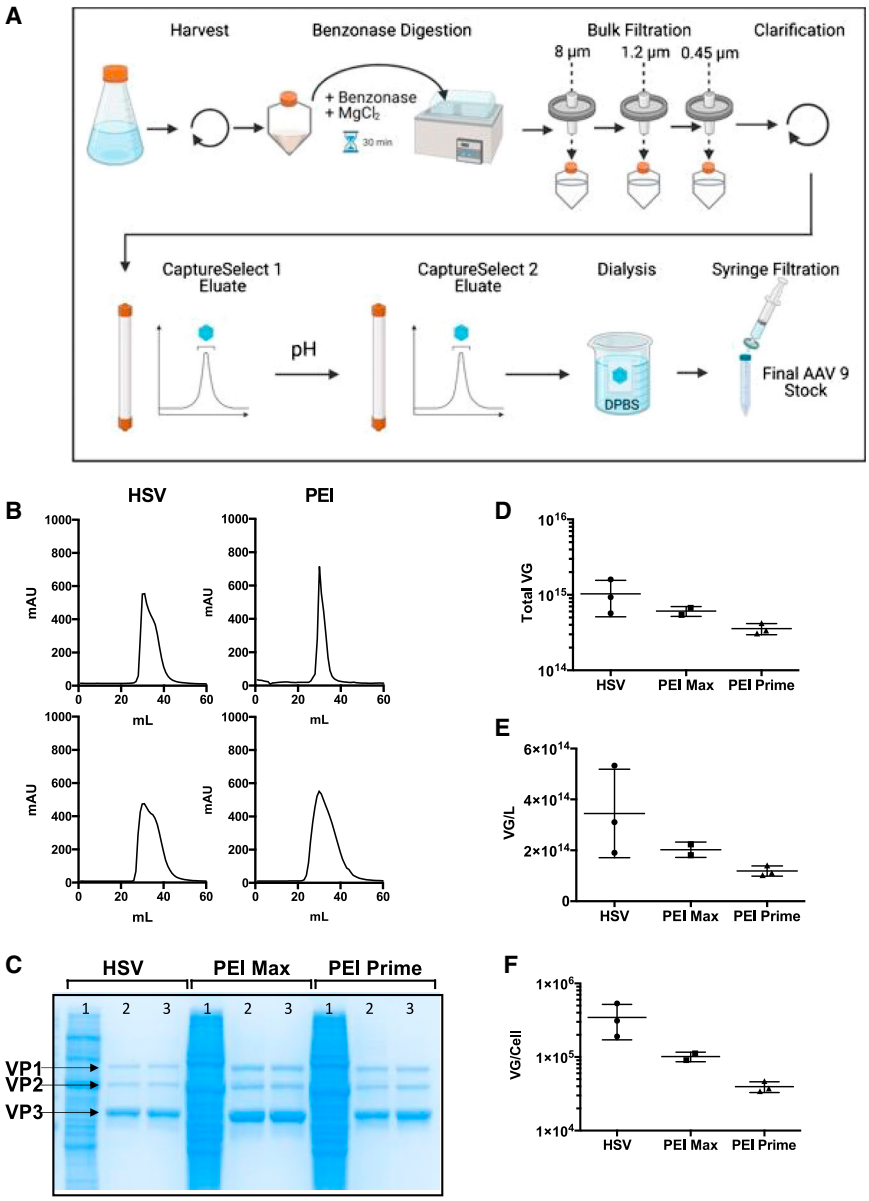

Figure 2. Downstream process characterization for large-scale production

(A) Downstream purification process flow chart. Chart depicts step-by-step flow for AAV9 purification from 3 L cell harvests. (B) Elution peaks. CaptureSelect elution chromatograms for HSV- (left) or PEI- (right) mediated AAV production, and for first (top) and second (bottom) captures. Absorbance unit (mAU) (y axis) versus volume in mL (x axis). (C) Sample purity assessment by Coomassie-stained protein gel. Same sample volumes were loaded for (1) benzonase-treated cell harvest, (2) first CaptureSelect elution peak, and (3) second CaptureSelect elution peak. One representative experiment of three for the HSV, PEI Max, and PEI Prime methods. (D) Total AAV9 vgs yield in cell harvests. Cells were harvested either 48 h after HSV infection or 72 h after PEI transfection, lyzed, and benzonase treated. The total vgs shown for each experiment (scatter dots) as well as average and SD for HSV-mediated production (n = 3), PEI Max- (n = 2) or PEI Prime-mediated production (n = 3). (E) Volumetric yields in upstream cell harvests. Same as (D) with total vg yield divided by the production volume (3 L). (F) Specific yields in upstream cell harvests. Same as (D) with total vg yields divided by starting cell numbers.

namely, the PEI-to-plasmid ratio, total plasmid DNA amount, cell concentration, and PEI/DNA-to-cell ratio. The molar ratio between pTRUF5 and pDG-UF9-KanR was set to equimolar (1:1) in all experiments. Cell harvests (72 h) and crude lysates were processed identically to those used for PEI Max. The yields obtained when using a PEI-to-DNA ratio of 2 or 3 were similar, and a ratio of 3 was selected based on the manufacturer's recommendations (Figure S1C). Next, we evaluated the starting cell density, varying from 1×10^6 to 4×10^6 c/mL, either with a constant amount of plasmid DNA or an amount proportionally increasing to the cell concentration. Contrary to PEI Max, the difference between 1×10^6 and 2×10^6 was more significant, with a three-fold increase in yield at 2×10^6 cells/mL (Figure 1G). Additionally, increasing the concentration to 3 or 4×10^6 cells/mL increased the overall yield, without the need to further increase the total DNA amount. The conditions for PEI Prime were set at 3×10^6 cells/mL and 75 µg total DNA for the rest of the study. When compared with the yields obtained with PEI Max, we noted a small but consistent increase with PEI Prime, reaching an average of 2×10^{14} vg/L (Figure S1D). The infectivity of rAAV9 produced with either PEI type was identical (Figure S1E).

Novel rAAV9 purification protocol suitable for both HSV and PEI production platforms

Our novel protocol was designed to enable rAAV9 purification from either HSV- or PEI-based upstream processes, to support scalability and to result in high purity. The protocol used the AAV9-specific POROS CaptureSelect AAV9 Affinity resin. Based on the data generated by the small-scale optimization studies, the rAAV9 vector was purified from the producer cells. The production scale for both HSV and PEI was set to a 3-L working volume. The complete step-by-step process is illustrated in Figure 2A and detailed in the materials and methods.

The experimental design for the comparison of the AAV vector production using HSV with the PEI transfection included the production and purification of three independent rAAV9-GFP vector stocks for each production method (HSV, PEI Max, and PEI Prime) for a total of nine lots, each purified using the same protocol described above and submitted to all analytical studies concomitantly to avoid the

impact of assay variability across lots. Each method used the optimal conditions defined for each production, which resulted in different cell densities, with HSV using the lowest cell density at 1×10^6 cells/mL,[22] PEI Max using 2×10^6 cells/mL, and PEI Prime using 3×10^6 cells/mL. Overall, we did not encounter any major differences between the HSV- and PEI-produced samples during the purification process, but we noted that the filtration steps were longer and more cumbersome for the PEI-generated samples and that the final clarification step by centrifugation resulted in thicker pellets. Additionally, the volumes of the column loads were higher for PEI runs and resulted in longer loading times. This was very likely caused by the greater cell number and protein loads generated from the PEI transfections. The transfection-generated pellets were visibly green, confirming a large excess of GFP protein expression, as compared with the HSV-infected cell pellets. The PEI-produced samples generated both higher elution peaks and area under the curve values than their HSV counterparts (Figure 2B), which also suggested a higher protein content in these samples and/or AAV9 capsids. This was orthogonally confirmed with Coomassie staining (Figure 2C), wherein the benzonase-treated cell lysates contained more proteins (lanes 1) and AAV capsids (lanes 2 and 3) in the PEI-produced stocks. The post-chromatography purity was similar across the methods (lane 3). Step-by-step recovery was also similar across the methods and runs and ranged between 30% and 60% after the second chromatography (Figure S2A). This confirmed that our purification platform worked equivalently with the two upstream methods.

The rAAV9 vector titers were assessed in the benzonase-treated harvests for each of the nine runs and averaged for each production method (Figure 2D). Overall, the HSV method generated higher rAAV9 vector yields than PEI, with an average of $1.03 \times 10^{15} \pm 5.22 \times 10^{14}$ total vg, approximately two- to three-fold higher than those obtained with PEI Max and PEI Prime, with $6.08 \times 10^{14} \pm 9.04 \times 10^{13}$ and $3.57 \times 10^{14} \pm 5.92 \times 10^{13}$ total vg, respectively. Of the three runs performed with HSV, one run was significantly lower than the other two, which resulted in a lower than expected average based on historical yields.[22] When the total vg yields were adjusted for volume and cell numbers, we obtained the volumetric yields (vg per liter of production volume) and specific yields (vg per starting cell number). The volumetric yield values reflected the same trend, with the HSV method averaging 3.45×10^{14} vg/L, or approximately 1.7- and 2.9-fold higher than PEI Max and PEI Prime, respectively (Figure 2E). The most significant difference between HSV and PEI production was the much higher specific yield obtained with HSV, resulting in 3×10^5 vg/cell, or a 3.4- to 8.7-fold increase when compared with PEI Max and PEI Prime, respectively (Figure 2F). This was the combined result of the higher yields together with a lower cell number used in the HSV platform. We noted a lower variability for all the PEI runs, suggesting strong reproducibility across batches. We also verified that the rAAV9 vector infectivity was not affected during the purification process, by analyzing the vg-to-TU ratio for each batch at three different purification steps, namely, the benzonased harvest and the eluates from each column chromatography step (Figure S2B). Despite a relatively high variability across the batches and across the conditions, the overall trend showed that the ratio diminished at each purification step, suggesting that particle infectivity improved as purity increased. This also confirmed that the infectivity was not negatively affected by the purification process.

HSV infection resulted in higher volumetric and specific yields than PEI transfection

The overall yields obtained for each method were compared across the nine fully purified rAAV9-GFP vector stocks (Figure 3A). HSV-generated vector yields were higher than those generated by either PEI method, with an average of 2.72×10^{14} vg per batch, two-fold more than obtained with PEI Max and 1.6-fold more than with PEI Prime. The transfection yields were similar with either PEI used. The average volumetric yield for HSV was $9.05 \times 10^{13} \pm 4.23 \times 10^{13}$ vg/L compared with $4.33 \times 10^{13} \pm 2.14 \times 10^{13}$ and $5.56 \times 10^{13} \pm 1.64 \times 10^{13}$ for PEI Max and PEI Prime, respectively (Figure 3B). The method with the lowest variability seemed to be PEI Prime. Again, the most dramatic difference between the infection and the transfection methods was observed when comparing the specific yields, with HSV generating close to 1×10^5 vg/cell, well in excess of PEI Max and PEI Prime (Figure 3C). This was further demonstrated by calculating the yield per biomass of cell harvest, with HSV resulting in an average of 9.50×10^9 vg/mg of cell pellet, versus approximately 2.10×10^9 vg/mg with PEI.

Next, we calculated the ratio of total vg over the total TU as an indication of the infectivity of our final stocks (Figure 3D). Both PEI reagents resulted in comparable, yet slightly lower, vg-to-TU ratios than with HSV infection.

Biochemical purity was evaluated by Coomassie staining of a protein gel where the same vg amount was loaded for each sample (Figure 3E). After quantification of each capsid protein (VP1, 2, and 3) and comparison with other proteins detected in the sample, we obtained an overall purity in excess of 99% with each stock. The difference in capsid load will be further discussed below.

PEI-generated vectors have significantly more empty capsids than HSV-produced vectors

When evaluating the overall biochemical purity by protein staining (Figure 3E), we noted a very significant difference in the capsid protein loads in samples generated by PEI transfection, which indicated an excess of empty capsids in these preparations, as compared with HSV-produced samples. To better quantify the total amount of capsids and the percentage of full capsids, we used three orthogonal analytical methods. First, we measured the total protein amount using the traditional bicinchoninic acid assay (BCA) or the Stunner, an instrument that utilizes a combination of UV/Vis concentration, dynamic light scattering (DLS), and static light scattering (SLS) to quantify both the vg titers and the capsid titers. PEI-generated samples contained an average five-fold excess of total proteins compared with HSV-generated samples, when standardized to the same amount of vg (Figure 4A). The percentage of full capsids (Figure 4B) was obtained using the vg titers and the total amount of capsids (Figure 4C)

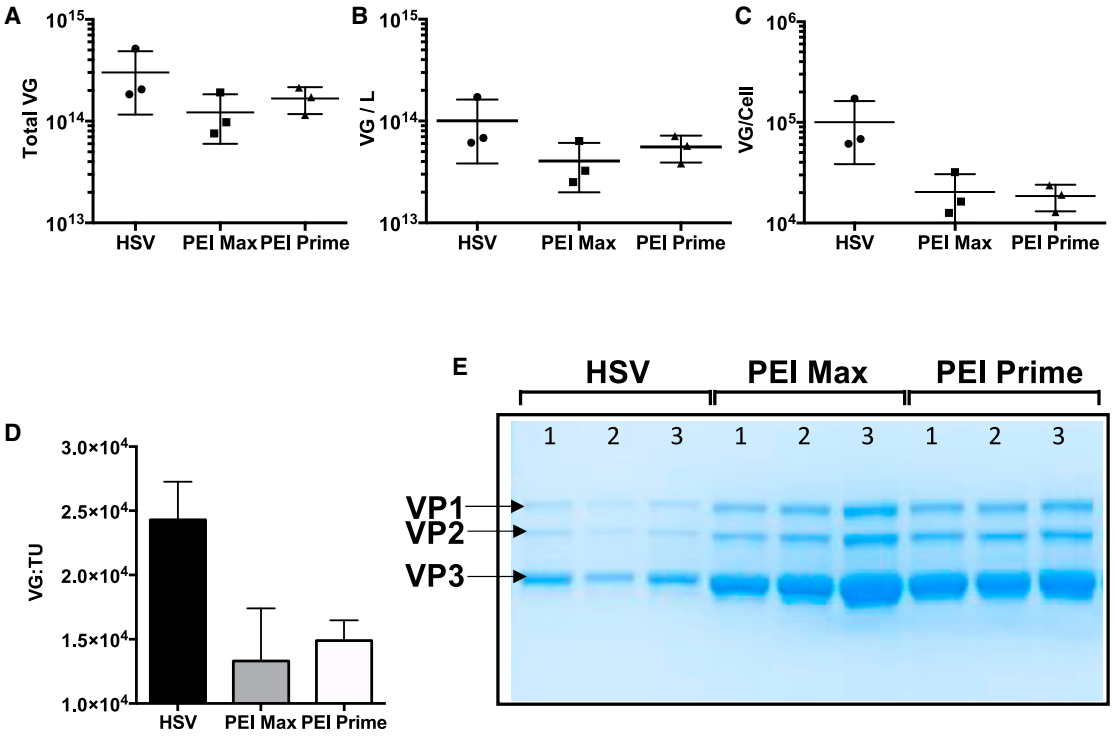

Figure 3. Vg yields in fully purified rAAV9-GFP vector stocks

(A) vg yields. vg titers and total yield were assessed for each large-scale 3-L production run in fully purified rAAV9 final stocks after dialysis in DPBS. Total vg shown for each experiment (scatter dots) as well as average and SD for HSV-mediated production (n = 3), PEI Max-mediated, (n = 3) or PEI Prime-mediated production (n = 3). (B) Volumetric yields in upstream cell harvests. Same as (D) with the total vg yield divided by the production volume (3 L). (C) Specific yields in upstream cell harvests. Same as (D) with the total vg yields divided by starting cell numbers. (D) Infectivity ratios for each production methods in purified rAAV9 vector stocks. TU titers were determined for each final rAAV stocks and used to calculated the vg-to-TU ratio as a measure of AAV stock potency *in vitro*. Average and SD for n = 3 for each production method. (E) Biochemical purity and capsid loads. Same amounts of vg (5×10^{10}) for each of the nine stocks were loaded on SDS-PAGE and stained for protein by Coomassie blue. AAV9 VP1, VP2, and VP3 identified according to their MW.

deducted from the protein concentrations. HSV-generated AAV9 vector stocks contained five times more full capsids, with an average of 28% full compared with 6% in the PEI-generated stocks. The data generated with the Stunner were very similar to the BCA, although more consistent across the samples. The difference across the two methods could be due to the slight difference noticed in vg titers when acquired by the Stunner, and compared with our quantitative polymerase chain reaction (qPCR) method (Figure S3A). Next, we performed a rAAV9 capsid ELISA. In all but one sample, the capsid concentrations were consistently higher when measured by ELISA then when assessed by BCA or Stunner, by almost two-fold. This resulted in 20%–40% lower values of full capsids (Figure 4B). Last, we conducted electron microscopy imaging on one representative batch of rAAV9-GFP produced by HSV and by transfection (PEI Max). Although much more variable than the other methods, the overall values confirmed the data obtained with the BCA and Stunner, with 32.16% ± 2.99% full capsids for HSV-produced rAAV and 10.53% ± 2.96% for PEI produced rAAV (Figure S3C). To visually illustrate these findings, the same amount of total proteins was loaded from each rAAV stock on a protein gel, resulting in nearly identical AAV capsid proteins detection for all the samples (Figure S3B).

These results were in line with our previous findings that the HSV method resulted in rAAV9 stocks with a higher amount of full capsids, with an average of 33.6% ± 8.81 (n = 5) than the rAAV9 stocks produced using the traditional calcium phosphate transfection method in adherent HEK293 (9.17% ± 7.96, n = 4) (unpublished data from study published in[21,22]).

PEI-generated vectors contain significantly more residual HCP than HSV-produced vectors

We assessed HEK293 HCPs by ELISA. The concentrations of HCP in HSV-made samples ranged from 6.52 to 18.87 ng/mL and from 40 to 500 ng/mL with PEI-made samples (Figure 4D). This difference was further emphasized upon standardizing the HCP amounts across the samples to 10^{12} AAV vg (Figure 4E), with HCP values 13- to 50-fold higher when AAV vector stocks were produced using PEI transfection versus HSV infection. We also noted that the samples generated using PEI Prime resulted in a two-fold higher residual HCP than with PEI Max. When standardizing the HCP to the total cell number, the differences remained detectable (Figure 4F). These data represented a significant improvement from previous rAAV9 vector preparations described

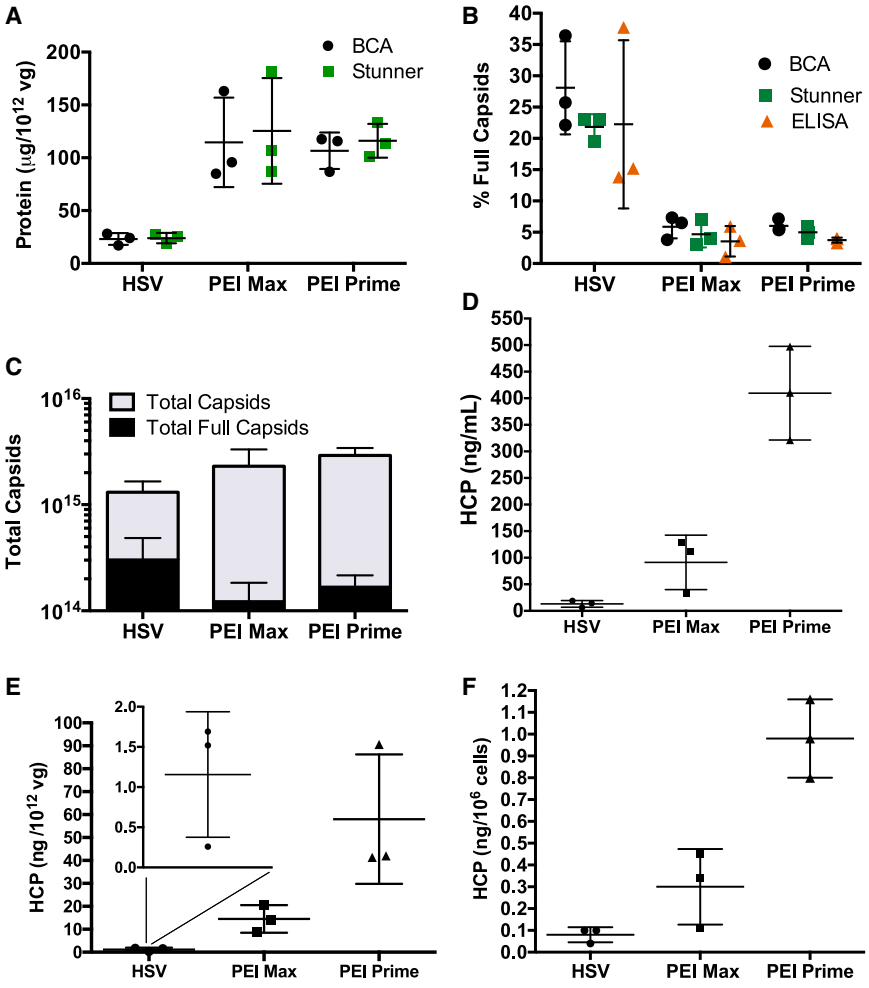

Figure 4. Comparison of full and empty capsid rates and residuals HCP in transfection- versus infection-produced rAAV9 vector stocks

(A) Total proteins. Protein concentration and total protein were determined using BCA or a Stunner instrument and standardized across the AAV batches to 10^{12} vg . Values obtained for each separate run (scattered dots) and average and SD calculated for three independent production batches for each of three productions method (x axis). (B) Percentage of full capsids. The percentage of full capsids was determined based on the total capsid titers obtained from the total protein concentration (BCA, black dots) or directly from the Stunner instrument (green dots) or by ELISA (orange dots), and the vg titers of each AAV stock. The values obtained for each separate run (scattered dots) average and SD shown for three independent batches and for each production method. (C) Total and full capsid titers. Total amount of capsid and full capsids shown for each production method. Averages and SD for three independent vector stocks per method. (D–F) Residual HCPs. Concentration of residual HEK293 HCPs determined by ELISA. The values obtained for each separate AAV vector stock (scattered data points) and average and SD shown for three independent stocks and for each production method. (E) Same as (D), with values standardized per 10^{12} vg for each AAV vector stock. Visual enlargement provided for HSV method owing to low values. (F) Same as (D), with values standardized for 10^6 cells.

in an earlier work, in which we obtained 3.58 µg/10^{12} vg ± 1.24 (n = 5 batches) for HSV-produced stocks and 10.43 µg/10^{12} vg ± 5.02 (n = 4 batches) for $CaPO_4$-prepared stocks (unpublished data from study published in[21,22]).

Altogether, our data showed that PEI-mediated transfection resulted in excessive residual HCP in AAV vector stocks compared with those produced using the HSV method. However, the amount of HCP in all AAV preparations remained extremely low and represented, at the maximum, 0.08% of total proteins, for a protein purity superior to 99.92% for all generated samples.

PEI-generated vectors contain higher residual host cell and AAV RepCap DNA

Next, we checked whether the production method could result in different residual host cell (HEK293) and helper AAV DNA contents. Host cell DNA residual was detected in all AAV final stocks. However, HSV-generated AAV stocks contained more than a 1-log lower amount of HC DNA than their PEI counterparts (Figure 5B). Both PEI methods resulted in a similar amount of HC DNA. HC DNA represented approximately 2 × 10^{-5}% of total AAV genome with HSV production and about 5 × 10^{-4}% for PEI production (Table 1).

The common residual AAV DNA for both methods consisted of sequences of AAV2 Rep and AAV9 Cap, provided either by rHSV or the helper plasmid. We quantified residual AAV DNA using real-time qPCR targeting one region in AAV2 Rep78 and one region in AAV9 Cap ORF (see Figure 5A). All samples were tested concomitantly for direct comparison. In the same experiment, we also evaluated whether the residual DNA was packaged or not by submitting the samples to DNAse I digestion before PCR. First, we observed that the DNAse digestion did decrease the overall copy number by approximately two- to three-fold in most samples (Figure 5C), suggesting that the majority of the residual plasmid DNA detected was packaged, or not sensitive to DNase I. Further, PEI-produced rAAV vector stocks contained approximately 5-fold more Rep DNA than HSV-produced samples, and a 10-fold excess in Cap DNA (Figure 5D). On average, PEI Prime resulted in a lower amount of residual Rep and Cap DNA than PEI Max. A summary of all residual DNA data is presented in Table 1.

HSV-generated AAV9 vector stocks contain inhomogeneous amounts of residual rHSV DNA

Determining the amount of residual HSV DNA by qPCR is a daunting task owing to the length and complexity of the

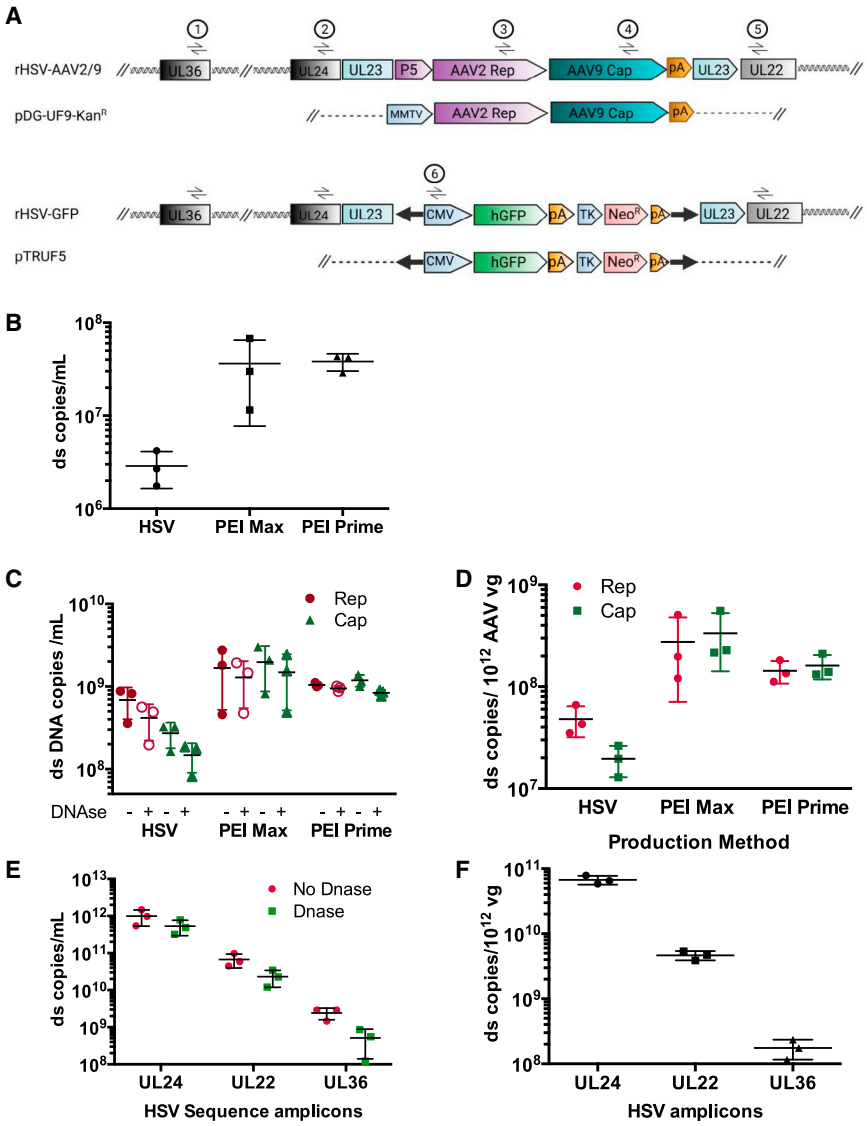

Figure 5. Comparison of residual DNA rates in transfection- versus infection-produced rAAV9 vector stocks and residual HSV DNA

(A) Diagram of HSV and plasmid constructs and PCR amplicons. Recombinant HSV and plasmid DNA aligned with major ORFs and regulatory sequences. PCR amplicons annotated as: ① UL36, ②UL24, ③AAV2 Rep, ④AAV9 Cap, ⑤UL22, and ⑥ CMV. Not at scale. (B) Residual host cell DNA. Copy numbers of HEK293 DNA obtained by ddPCR for each AAV stocks and averaged/SD for three independent stocks. (C) Residual AAV helper DNA. Real-time qPCR targeting AAV2 Rep (scattered red dots) or AAV9 Cap ORF (scattered green triangles), with or without to DNase 1 treatment (±). The Ds copies numbers obtained for each separate AAV vector stock for each production method and averaged/SD for three independent stocks. (D) Residual AAV helper DNA. Ds copies numbers standardized to 10^{12} vector copies. Values obtained for each separate AAV vector stock for Rep (scattered red dots) and Cap (scattered green squares) shown for each production method and average and SD for three independent stocks. (E) Residual HSV DNA. Real-time qPCR targeting HSV UL24, UL22, and UL36 with (scattered green dots) or without (scattered red dots) DNase 1 treatment. The ds copies numbers obtained for each separate AAV vector stock for each production method and averaged/SD for three independent stocks. (F) Residual HSV DNA. Ds copies numbers standardized to 10^{12} vector copies (n = 3 independent stocks).

viral genome. The data reported here are for information only and for direct comparison across the production methods. We selected three pairs of primers targeting two HSV regions near the AAV ITRs in the HSV genome backbone (UL24 and UL22) and one region located more than 30 kb away from the AAV cloning junctions (UL36) (Figure 5A). The UL24 and UL22 target concentrations could be determined using the same standard curve used to determine the Rep and Cap DNA concentrations. UL36 was determined using a purified HSV genome, and a direct comparison with UL22 and UL24 should, therefore, be taken with caution. DNase I digestion resulted in a small decrease in HSV DNA (Figure 5E). HSV DNA was detected in all rAAV stocks, yet highly variable across the targeted regions (Figure 5F), with the highest values obtained within UL24, and the lowest within UL36 (Table 1).

PEI-mediated transfection results in higher Rep and Cap protein expression

We initiated a side-by-side time course to study the levels of Rep and Cap gene expression during HSV versus PEI transfection production runs. In these small-scale experiments, the same concentration of cells was used both in infection and transfection to ensure comparability. Expression levels were analyzed by Western blotting using specific antibodies at various time points during the production cycle (Figure 6A). Rep 52 and 78 were detected at significant levels as early as 8 h after PEI transfection and in large excess at 48 h after transfection. In the HSV production setting, Rep proteins were detected at 16–24 h after infection. At each time points, but especially at 24 and 48 h, the level of Rep78 and 52 expression remained in excess in the PEI-transfected cells compared with the HSV-infected ones and were superior to the levels seen for Rep 68 and 40.

Similarly, PEI transfection resulted in a higher expression of all three capsid genes, VP1, 2, and 3, with detectable levels observed after 14 h and the maximal levels after 48 h (Figure 6A). Detectable levels of Cap gene expression were found 16–24 hours after HSV infection and were significantly lower than in PEI-transfected cells at 48 h.

Table 1. Residual DNA in rAAV9 stocks

	Percentage residual DNA to AAV genome					
Production method	HC DNA	Rep	Cap	UL24	UL22	UL36
HSV	$2.19 \times 10^{-5} \pm 1.16 \times 10^{-5}$	0.005 ± 0.002	0.002 ± 0.001	6.75 ± 1.03	0.47 ± 0.07	0.02 ± 0.01
PEI Max	$6.27 \times 10^{-4} \pm 5.39 \times 10^{-4}$	0.028 ± 0.02	0.033 ± 0.019	NA	NA	NA
PEI Prime	$5.08 \times 10^{-4} \pm 7.04 \times 10^{-5}$	$0.014^{-2} \pm 0.004$	0.016 ± 0.004	NA	NA	NA

Residual DNA measured by ddPCR (HC DNA) or qPCR (all others) and percentage of residual DNA in copy number calculated versus AAV genome copies. Data represent the average obtained from 3 AAV stocks and standard deviation. NA, not applicable.

Kinetic of AAV genome replication is different in PEI-transfected cells compared with HSV-infected cells

In parallel with the gene expression kinetic study, we analyzed the replication levels of the AAV vg in the two production platforms. AAV replication forms (RF) were extracted from transfected or infected cells at various time point and analyzed by Southern blotting (Figure 6B). Interestingly, the pattern of AAV genome replication was reversed to that observed for Rep and Cap expression: HSV-infected cells showed higher and earlier levels of AAV RFs at all time points, starting at 14 h after infection and increased significantly by 24 h. Levels at 24 and 48 h were similar, in line with our previous studies showing that AAV vector yields are similar in harvest at 24 or 48 h after infection.[22] By 48 h after transfection, the level of AAV monomeric RF had reached a similar level to that observed in the HSV samples, but the levels of dimeric and multimeric RFs remained lower in PEI-transfected cells. Another important observation was that the levels of single-stranded AAV genomes remained significantly higher in HSV-infected cells.

DISCUSSION

In this work, we demonstrated that our newly implemented production platform, using suspension-adapted HEK293 and PEI-based transfection, combined with our novel AAV9-specific purification process, resulted in rAAV9 vector stocks of high titers, high purity, and high potency. Our new platform provides an efficient and scalable process that outcompetes, both in yield and in quality, our standard calcium phosphate transfection method in adherent HEK293.[22] PEI is a popular reagent used for rAAV vector production from laboratory to clinical scale.[2,15,16] We found that, for PEI Max, our parameters were in line with previously published works: a PEI-to-DNA ratio of 2:1, equimolar ratio of helper to AAV plasmid, 1.5 μg DNA/mL, 2×10^6 cells/mL concentration, and a 72-h harvest.[15,16,25–27] The conditions with PEI Prime were slightly adjusted for a PEI-to-DNA ratio of 3 and a cell concentration of 3×10^6 cell/mL. To our knowledge, rAAV production with PEI Prime has not been reported as of yet. Of note, many published protocols use a triple transfection[15,16,25] rather than a double transfection like in our work.[27]

Deciding on a production method for rAAV remains a difficult choice, with several options to choose from, most with advantages and disadvantages. Comparison across the methods is often challenged by the impact of various downstream processes, as well as analytical methods across laboratories. For this reason, we believe that it is important to conduct true side-by-side comparison studies across the upstream platforms. Previously, we had reported side-by-side data comparing the calcium phosphate transfection in adherent HEK293[21] and the HSV production system in adherent or suspension-adapted HEK293.[22,23] From both studies, the HSV platform in suspension was found superior and resulted in higher yields. Paulk et al.[28] recently presented a side-by-side comparison of the PEI-transfection in HEK293 platform with the Baculovirus expression system (BEV) in insect cells, and demonstrated significant differences in the post-translational modifications of the AAV capsid, the percentage of full capsids, and the virus potency. In the current work, HSV yields of 3–4 $\times 10^{14}$ vg/L were again found to be superior to the PEI-mediated ones by at least two-fold, and far exceeded transfection-generated specific yields by up to five-fold (>3 $\times 10^5$ vg/cell). Our volumetric yields in bulk harvests ranged between 1 and 2 $\times 10^{14}$ vg/L after transfection, with a specific yield as high as 1.1 $\times 10^5$ vg/cell. These yields remain highly competitive with yields reported from other laboratories (1 $\times 10^{13}$ to 2 $\times 10^{14}$ vg/L),[16,29] as well with other methods such as the BEV system[30] or the HSV infection method using suspension-adapted BHK.[20]

Our current work also included a new downstream purification protocol that increased the quality of our rAAV9 stocks and the overall vector recovery. It is worth noting that we purified the cell-bound vector particles rather than media released, which constitutes a notable difference with protocols currently used in the industry. The impact of a total harvest and lengthier production cycles on the virus yield and on the particle potency[15,16,28,31] and perhaps on the ratio of full versus empty particles[32] needs to be further evaluated. Our purification process is simple and robust. Our overall process recovery from start to finish ranged from 30% to as high as 50% of the total vector mass, and the rAAV9 particles potency was not affected. Based on our vg and capsid data, we estimated that the capacity of the CaptureSelect AAV9 resin reached 1.6 $\times 10^{14}$ vg/mL and 6 $\times 10^{14}$ capsid/mL. According to the manufacturer, this resin's capacity is approximately 1 $\times 10^{14}$ vg/mL.[29,32,33] In line with the findings obtained on pre-purified stocks, we confirmed that the purified AAV9 vector yields generated by HSV co-infection (6 $\times 10^{13}$ to 1.7 $\times 10^{14}$ vg/L) remained superior to the ones generated with PEI (2–6 $\times 10^{13}$ vg/L). However, both HSV and PEI-generated rAAV9 purified stocks proved competitive with other published works that report volumetric yields from 1 to 5 $\times 10^{13}$ vg/L for the transfection in

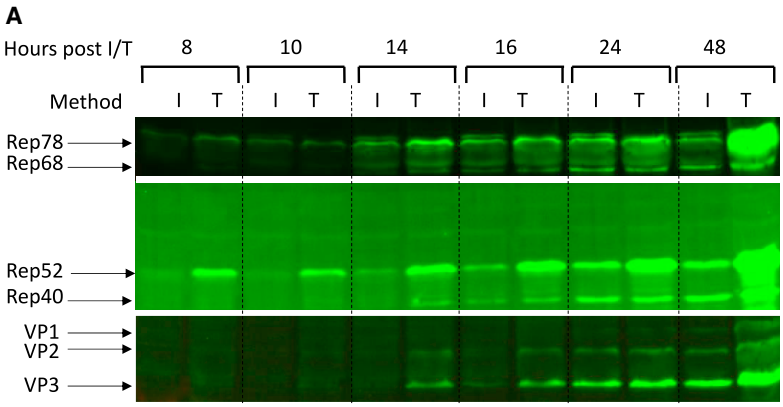

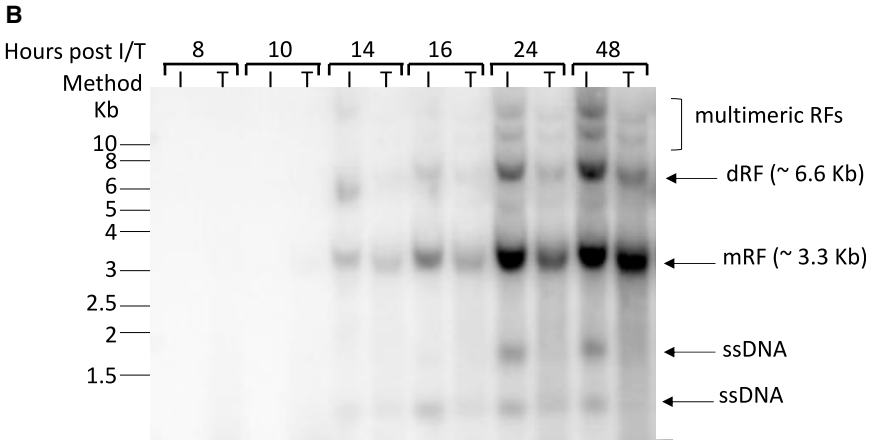

Figure 6. AAV genome replication and proteins expression in transfected and infected cells

(A) Expression level and kinetics of Rep and Cap expression. HEK293 were transfected or infected and protein lysates was prepared for Western blot analysis at various times after production initiation. Rep and Cap were detected by western blotting followed by antibody detection. One representative experiment. HEK293 (B) replication levels and kinetics of AAV genome. HEK293 were transfected or infected and cell lysates was prepared according to Hirt's extracts protocol at various times after production initiation. AAV genome was detected after membrane transfer by Southern blotting and a ^{32}P-CMV labeled probe. RF, replicative form; m, monomeric; (D), dimeric; ssDNA, single-stranded AAV DNA (n = 1 representative experiment).

suspension HEK293[16] or HSV system in suspension BHK[34] and the BEV system.[30,35]

The heightened stringency to meet the FDA guidelines for high levels of purity and quality, including potency, of clinical rAAV drug products often outcompetes with the overall process recovery or the particle potency. In this work, we present data for the detection of product- and process-derived impurities. In earlier works, we and others have shown that the HSV platform generated rAAV stocks of similar or higher infectivity than transient transfection.[21–23,36,37] In the current work, the infectious titers reported for the PEI method were similar or higher than the ones found with the HSV method, which was a great improvement from our previous calcium phosphate transfection data. This suggest that perhaps the suspension format, combined with a different transfection reagent, is more favorable to rAAV production and potency. It does, however, emphasize the need to characterize each rAAV parameters for each platform model and the reagents used for their impact on the quality and potency of the AAV preparations produced.

Our data convincingly showed that the HSV platform was more efficient at producing full rAAV9 capsids than the transfection platform. Our transfection-produced rAAV lots contained less than 10% of full capsids in final stocks, which was consistent with values obtained with rAAV produced by calcium phosphate transfection in adherent HEK293. Low amounts of rAAV full capsids have been commonly observed with transient transfection, although with a wide range across the studies (1%–30%)[16,38] and in clinical batches.[39] In contrast, an increase in AAV full capsids has been reported for AAV 1 when using the HSV method, and for AAV9 as shown in this work.[21,22,37]

Residual HEK293 HCPs, a process-derived type of impurities, were detected in all our rAAV vector stocks, but the rate was decreased by more than 1 log in the stocks produced by HSV, with an average of 1 ng per 1×10^{12} vg, and compared with PEI-produced stocks, containing 15 to 60 ng per 1×10^{12} vg on average. HCP content superior to 3 ng per 1×10^{12} vg have been reported in previous clinical rAAV1 produced by HSV.[34,37] The higher cell number used for our PEI-based protocols would support the higher HCP content in these stocks, but it fails to fully justify this excessive increase in HCP content. It is possible that the purification process may be slightly less efficient owing to a higher burden of proteins generated by PEI transfection, both in HCP and empty capsids. Our data confirm that our newly implemented purification protocol resulted in AAV9 vector stocks with a significantly increased quality with low HCP content compared with other platforms.[28,29,38]

Unsurprisingly, residual amounts of plasmid DNA were detected in all of our transfection batches, and residual amounts of HSV genomic DNA, in all of the infection batches. For the purpose of our comparison, two sets of amplicons were designed within AAV2 Rep and AAV9 Cap sequences, the only common denominator between the transfection (helper plasmid) and the infection (helper rHSV) stocks. In transfection-made stocks, we found that Rep/Cap DNA residuals constituted approximatively 0.01%–0.06% of the total AAV vg, with

no significant difference between Rep and Cap, or PEI Max versus PEI Prime. However, the levels of Rep/Cap were significantly decreased in the samples generated by HSV, representing 0.001%–0.007% of the total AAV DNA, or 10–15 times lower than in their transfection counterparts. Since the presence of DNA was detected after DNAse I digestion, it does suggest that these impurities were either packaged or inaccessible and, therefore, protected from the nuclease activity, as suggested by others.[40] Illegitimate packaging into AAV capsids has been well-studied across the manufacturing platforms (as reviewed in[29,38]). Rep/Cap Packaging rates between 0.04% and 0.1% have been reported for the BEV platform and between 0.01% and 0.4% for the triple transfection. The values obtained in the AAV stocks produced by HSV see to be significantly lower than in other systems, including HSV from previous published works.[41] The difference in Rep/Cap residual DNA between HSV and transfection may be the result of the 4-log differences in the copy number of Rep/Cap DNA introduced in the cells by transfection (approximately 2×10^4 copies/cell) compared with the very low amount introduced by infection (4 copies/cell), and the absence of AAV ITRs on the helper virus (see below).

Although not a part of a direct comparison with the transfection process (we did not assess residual plasmid backbone beside RepCap regions), we also reported values for HSV DNA residuals detected in our three HSV-produced stocks. We found log differences between the amounts of residual HSV DNA depending on the location on the recombinant HSV genome. The lowest amount was found for UL36 (0.02%), located more than 33 kbp from the AAV junction. An average of 0.47% was found for UL22 and 6.75% for UL24. Both UL22 and UL24 amplicons are located in regions closely located to the AAV ITRs, approximately 0.7 kbp upstream of AAV 3′ ITR (right) for UL24 and approximately 0.9 kb downstream of AAV 5′ ITR for UL22. Illegitimate packaging of helper virus or helper plasmid DNA has been demonstrated and described to great extent for other production platforms (reviewed in[29,38]). For transfection-based methods, the plasmid residual was detected as high as 6% of the total vector DNA.[38] Rates as high as 2% of baculovirus DNA were detected in BEV-produced AAV,[40] and higher than in HEK293 as shown in a side-by-side comparison by Paulk et al.[28] In all studies, it was shown that DNA fragments from across the helper plasmid(s) or virus DNA can be detected to various levels in AAV stocks, including in clinical and commercial grade AAV stocks.[40] Further, the proximity of AAV ITRs significantly increases the rate of illegitimate packaging, which can enable reverse, or bidirectional, packaging, and both ITR mediate different rates of reverse packaging.[40] For instance, Penaud-Budloo et al.[40] showed that as much as 11% of the gentamycin sequence can be detected in BEV-produced AAV owing to the proximity to the 3′ ITR. Our data support this finding, showing a higher detection rate for UL24, located upstream of the 3′ITR, than for UL22, located downstream of the 5′ ITR. This mechanism may also explain why residual HSV DNA is present in much higher amount than Rep and Cap DNA, since they are located on an HSV backbone that does not contain AAV ITRs. While our study did not assess the size nor potential transcriptional activity from HSV detected sequences, Ye et al.[41] published a detailed clearance study on illegitimate packing of HSV fragments in AAV stocks. They obtained a very similar rate than ours for UL36 (0.01%), and detected HSV DNA fragments ranging in size from 0.8 to 4.2 kb, that did not illicit any transcriptional activity.[41] Last, our replication study shows that the recombinant AAV-GOI genome is a coherent species migrating uniformly at the expected recombinant genome size, suggesting that the HSV DNA sequences are not co-linear to the rAAV genome. Our data strongly highlight that in-depth assessment and characterization of residual HSV DNA in clinical lots is critical.

Finally, in the last part of our study, we compared whether production by transfection or infection could modulate both the rate and/or the kinetics, of both the rAAV-GOI replication and AAV Rep and Cap protein expression. We found that the levels of Rep and Cap expression remained higher in the transfection setting than in the HSV one, and were detected earlier. Of note, Rep expression is driven by the mouse mammary tumor virus (MMTV) promoter in pDG-UF9-KanR and by AAV2 P5 in the HSV helper. Further, as mentioned earlier, Rep-expressing plasmid is introduced at a 4-log higher amount by transfection. Inversely however, the HSV co-infection method resulted in an earlier and more productive replication of the AAV vg. Altogether, our data highlight a series of biological attributes created by the HSV infection that create a favorable cellular environment to enable successful rAAV genome replication and packaging, resulting in high titers and a higher rate of full capsids. These findings provide a strong road map for the further development of helper plasmids and transfection designs that would mimic the HSV-triggered cellular environment.

While the HSV method seems to outcompete with TFX method on several key parameters, including higher titers, higher packaging rates, and lower impurities, the transfection method in suspension format presented in this work presents with clear advantages over our previous protocol in an adherent system, with AAV9 stocks produced at higher yields, higher potency, and higher purity in a highly scalable format.

MATERIALS AND METHODS

Cell lines

Expi293F were purchased from Thermo Fisher Scientific and were maintained in Expi293 Expression Medium (Thermo Fisher Scientific). Cells were carried in disposable shaker flasks from Corning (cat # 431143) at 5% CO_2, 37°C, 125 rpm, and 75% humidity in Multitron shaker incubators (INFORS HT). Cell concentration was maintained between approximately 5×10^5 cell/mL and 5×10^6 cell/mL during passaging. V27 cells (originally obtained from Dr. Knipe, Harvard University) and C12 cells (obtained from Dr. P. Johnson, Children's Hospital of Philadelphia) were maintained in DMEM supplemented with 5% FBS and 50 μg/mL Geneticin (Sigma). V27 are a stable derivative of VERO cells containing the expression cassette for HSV I ICP27.[42] C12 are a stable derivative of HeLa cells containing AAV2 Rep/Cap genome sequence to support genome replication of AAV2 ITR-containing rAAV vectors.[43]

Plasmids

Plasmid pTR-UF5 and pDG-UF9-KanR were used for rAAV9-GFP production by transfection and were produced at research grade at Aldevron, LLC, Fargo. Stocks were concentrated at 1 mg/m with endotoxins levels <100 EU/mg). Plasmid pTR-UF5 contains an AAV2-ITR vg cassette for the expression of humanized GFP under the CMV promoter.[21] Production was performed in Sure *E. coli* to maintain AAV2 ITR integrity. Plasmid pDG-UF9-KanR contains the AAV2 rep and AAV9 capsid ORFs under the MMTV and AAV2 P19/P40 promoters, respectively, as well as the Ad5 helper genes. Briefly, pDG-UF9-KanR was created by ligating the AAV2 Rep and AAV9 Cap sequences from plasmid pMA-P5-Rep2/Cap9 into pDG-KanR using Sal I and Cla I.[21] Plasmid pDG-KanR is a derivative of pDG[11] in which AmpR was replaced by KanR. Plasmid pHSV106-AAV2/9 derivation was previously described in[21] and consists in the P5-AAV2 Rep-AAV9 Cap sequences inserted into pHSV106-multiple cloning site, a shuttle plasmid that contains the HSV-1 thymidine kinase (TK) orf and surrounding regions, and a multiple cloning site within the TK sequence (depicted in Figure S4A). Plasmid was produced using Qiagen Endo-free maxi preparation kit (cat # 12362, Qiagen LLC) and concentration measured by nanodrop for use as a plasmid standard curve in the real-time qPCR assays as described below.

Cell concentration

Cell counts and viability were assessed using Countess II Automated Cell Counter (Thermo Fisher Scientific). For all production experiments, a minimum of 6 individuals cell counts and viability (countess II disposable slides) were performed and averaged. Cell viability superior to 90% was required.

rHSV production

rHSV-GFP was created by introducing the complete recombinant vg of rAAV2-UF5 within the genome of HSV type 1 deletion mutant d27.1. AAV2-UF5 contains the wtAAV2 ITRs, the CMV enhancer/promoter, and the humanized GFP coding sequence (described in detail in[21]). Helper recombinant HSV-AAV9 contained the entire expression cassette of AAV2 Rep and AAV9 Cap, under their respective endogenous promoters, as described in.[21] Production of recombinant herpes viruses rHSV-GFP and rHSV-AAV9 stocks was performed by infecting V27 cells in 10-layer CellSTACKs (Corning) at an multiplicity of infection (MOI) of 0.15 pfu/cell. At 72–96 h after infection, cells were lysed in 0.6 M NaCl (Lonza), harvested, and cell debris removed by centrifugation. The rHSV-containing cell lysate was concentrated by tangential flow filtration using TangenX Sius-300 kDda (Cat # XP300L01L, TangenX, Shrewsbury, MA). rHSV stocks were stored frozen at −80°C in 5% glycerol (Thermo Fisher Scientific).

Recombinant AAV viral vector production

Small-scale AAV production by transient transfection

Small-scale transient transfections were performed in Expi293 cells (50 mL production volume) in 125-mL shaker flasks (cat # 431143, Corning Inc.) using PEI MAX 40K (transfection grade linear PEI Hydrochloride, High potency linear, MW 40,000, cat # 24765-1, Polysciences Inc.) or PEI Prime (polyethyleneimine hydrochloride transfection grade, 1 mg/mL, Sterile-filtered, pH neutralized, cat # Prime-AQ100-100 mL, Serochem). PEI Prime was kindly provided free of charge by Serochem for this study. The PEI MAX stock solution was prepared at 1 mg/mL at pH 7.0 in water for injection (WFI, Hyclone cat # SH30221, Cytiva Lifesciences) and sterile-filtered. Aliquots were stored frozen at −80°C. For each transfection with PEI Max or PEI Prime, one DNA-containing solution (1.25 mL) and one PEI-containing solution (1.25 mL) were prepared in cell culture medium, combined, and incubated at room temperature for approximately 15 min before being added to the cells. All plasmid amounts were calculated based on the desired molar ratio and total DNA amount and are indicated for each experiment as the molar ratio between pTRUF5 and pDG-UF9-KanR (example 1:1). Unless otherwise indicated, cells were incubated for 72 h before harvest at 37°C, 5% CO_2, 75% RH, and 125 rpm. At the time of harvest, cells were spun down (2,000 rpm, 4°C, 20 min, Sorvall ST-40R, Thermo Fisher Scientific), rinsed in 1× DPBS (Hyclone, Cytiva Lifesciences), and spun down again. When required, the spent media were collected and stored frozen. Cell pellets were resuspended homogenously in 5 mL lysis buffer (50 mM Tris, 150 mM NaCl, pH 8.5) and subjected to a series of three freeze-thaws. Lysates were then digested with Benzonase (EMD Millipore) digestion (100 U/mL, 30 min, 37°C) and clarified by centrifugation (3,700 rpm, 20 min, 4°C, Sorvall ST-40R). Crude lysates were stored at −80°C for the duration of the study.

Unless otherwise specified, all small-scale production runs were performed as biological replicates. Infection runs were repeated independently (n = number of independent experiments, shown in the figure legends). Within each run, all the conditions were processed and assessed concurrently to provide paired data between the various conditions. Values obtained for each biological replicate were averaged and the standard deviation calculated as indicated in the figures' legends.

Large-scale production

Production of rAAV9-GFP by transfection with PEI Max. Expi293F cells were seeded in 5 L Corning Erlenmeyer cell culture flasks with vented cap (cat # 431685, Corning Inc.) at 2×10^6 cell/mL in 3 L final culture volume (for a total of 6×10^9 cells at initiation). In a first 250 mL conical tube, a total of 4.5 mg of plasmid DNA (pTRUF5, 0.969 mg and pDG-UF9-KanR, 3.531 mg for a molar ratio of 1:1) was added to cell culture media for a final volume of 75 mL. In a second conical tube, 9 mg of PEI Max (9 mL) were added to 66 mL of cell culture media (final volume 75 mL, for a PEI-to-DNA ratio of 2:1). The content of both tubes was mixed and incubated for approximately 15 min at room temperature before be added to the cell-containing shake flask.

Production of rAAV9-GFP by transfection with PEI Prime. Expi293F cells were seeded in 5 L Corning Erlenmeyer cell culture flasks with vented cap (Corning Millipore-Sigma cat # 431685) at 3×10^6 cell/mL in 2.85 L final culture volume (for a total of 9×10^9 cells at

initiation). A total of 4.5 mg of plasmid DNA (pTRUF5, 0.969 mg and pDG-UF9-KanR, 3.531 mg for a molar ratio of 1:1) was added to cell culture media (final volume 75 mL) and 13.5 mg of PEI Prime was added to a second tube containing cell culture media (final volume 75 mL, for a PEI-to-DNA ratio of 3:1), mixed with the DNA-containing mix and incubated for approximately 15 min at room temperature before being added to the cell-containing shake flask.

Production of rAAV9-GFP by rHSV co-infection. Expi293F cells were seeded in 5 L culture flasks at 1×10^6 cell/mL in 3 L final culture volumes (for a total of 3×10^9 cells at initiation). Cells were co-infected at a MOI of 2:4 with rHSV-GFP and rHSV-AAV9, respectively, in the presence of 60 mM NaCl (run # 3) or 40 mM KCl supplementation (run # 1 and 2).[23]

Cells were harvested after 2 (HSV infection) or 3 (PEI transfection) days incubation at 37°C, 5% CO_2, 75% RH, and 100–125 rpm. The 3 L harvest was transferred to 6 × 500 mL Conical tubes (Corning) and cell were spun down at 2,000 rpm, 4°C, for 20 min (Sorvall ST-40R, Thermo Fisher Scientific), rinsed in 500 mL 1× DPBS (HyClone, Cat # SH3002802), combined into one or two tubes and spun down again. The pellet weight was measured and the pellets were stored frozen until further processing.

Recombinant AAV viral vector purification

The rAAV manufactured by both infection- and transfection-based protocols were subjected to same purification protocol, depicted step by step in Figure 2A. The pellets were thawed at 37°C and homogenously resuspended in WFI with constant flushing for 5 min at room temperature. The solution was buffered by adding 2 M Tris-Cl pH 8 to obtain 25 mM Tris. Digestion of non-packaged cellular, viral, and plasmid DNAs and RNAs was performed by adding 50 U/mL Benzonase (EMD Millipore) and 1 mM $MgCl_2$, for 1 h at 37°C. The digested cell lysates were then clarified by centrifugation (27,000 g, 20 min, 4°C, Sorvall ST-40R, Thermo Fisher Scientific) followed by a three-steps filtration using 8-, 1.2-, and 0.45-μm PES filters (Polyethersulphone membranes, Cat # PES8047100, PES1247100, PES4547100, Steriltech Corp). Sodium chloride solution (5 M NaCl, AccuGene, Lonza) was added to the filtrate at 150 mM final and stored frozen at −80°C. The pH of the virus-containing load range between 7.4 and 7.81 across the runs. Viral particles were purified using a two-step chromatography approach. First, the virus-containing supernatant (affinity load) was loaded onto a sanitized and pre-equilibrated POROS CaptureSelect AAV9 Affinity resin (10 mL column volume, Cat # A36739, Thermo Fisher Scientific) pressure-packed in Vantage-L Laboratory column VL 11 × 250 (Cat # 96100250, Millipore) and pre-equilibrated with buffer A (25 mM Tris, 150 mM NaCl, pH 8 ± 0.5) and buffer B (100 mM citric acid, 100 mM arginine, pH 2.5 ± 0.2). The virus was eluted as a discreet peak (affinity eluate) at 80% buffer B or a pH of approximately 3.5. The eluate was subjected to second re-capture on the affinity column after diluting 1:6 in buffer A, and adding $MgCl_2$ (0.6 mM final), NaCl (150 mM final), and 1 M Tris, pH 10. The pH of the second affinity load ranged between 6.99 and 7.77 across the runs. The virus was eluted as a discreet peak (affinity eluate, 80% buffer B) at a pH of approximately 3.5, sterile filtered with Millex-GV syringe filter, 0.22 μm (Cat # SLGV033RS, EMD Millipore) and stored frozen at −80°C (eluate 2 sample). The final eluate was formulated in 1× DPBS (cat # SH30028.03, HyClone, Cytiva) by dialysis using 10K Slide-A-Lyzer Dialysis cassettes (Cat # 66456, Gamma Irradiated, 10,000 molecular weight cut-off, 12–30 mL, Thermo Fisher Scientific) following the manufacturer's instructions. Briefly, the samples were dialyzed at room temperature in 4 L DPBS over three consecutive buffer exchanges for 4 h, approximately 16 h or overnight, and 4 h, respectively. Upon completion the samples were sterile filtered with Millex-GV syringe filter, 0.22 μm (Cat # SLGV033RS, EMD Millipore) and stored at −80°C.

rAAV-specific assays

Vector genome titer

The vg titers were obtained by quantitative real-time qPCR as previously described[22] using primers UF5-3F (5′-CCAGGTCCACTTCG CATATT-3′) and UF5-3R (5′-GCGTGCAATCCATCTTGTTC-3′) (IDT) and plasmid pTR-UF5 for the standard curve established over a 10-fold dilution series from 1 ng to 1 fg and converted in copy number of double-stranded DNA to calculate vgs. Before amplification samples were treated with 10 U DNAse I (DNase I recombinant RNAse-free solution, cat #04716728001, Roche Applied Science) for 30 min at 37°C. Samples were serially diluted over a five-fold series between 5×10^2- and 1.56×10^6-fold. The PCR mix was obtained by mixing each primer (200 nM final) with 1× of SYBR Green (2× iQ SYBR Green Supermix, cat #170-8880, Bio-Rad), 2 μL of each sample dilution and water up to 25 μL per well (Ultra-Pure Distilled Invitrogen cat #10-977-015, Thermo Fisher Scientific). Cycling conditions were 95°C for 10 min and 40 cycles at 95°C 10 s and at 62°C 30 s (CFX Connect, Bio-Rad).

Transduction assay

Ad5-infected C12 cells (MOI of 20) were transduced in 96-well plates by serial dilutions of the rAAV-containing samples. After 42–48 h, GFP-expressing cells were visually counted under microscope and UV light, and the titer was calculated based on the sample dilution and volume.

AAV purity and VP ratio by Coomassie staining SDS-PAGE

Samples were prepared in WFI according to the desired volume and mixed with 1× final reducing sample buffer (5× reducing sample buffer, cat # PI39000, Thermo Fisher Scientific). Capsid denaturation occurred during a 5 min incubation at 95°C in a heat block. Denaturated samples were loaded in duplicate on 2 identical 10% Criterion Tris-HCl Precast gels (Criterion, cat # 3450009, Bio-Rad) and electrophoresis was conducted in Tris-glycine running buffer (10× Tris-Glycine-SDS buffer, cat # 1610732, Bio-Rad) at 100 V for 2–3 h. Protein detection was performed by Coomassie staining (GelCode Blue Stain, cat # 24590, Bio-Rad) and band intensity and quantification were performed on gels scanned on GelDoc EZ Imager (Bio-Rad) and analyzed with Image Lab software (5.2.1). Volumes calculated by the software were used to calculate the ratio between VP1, 2, and 3. The software-generated percentage of detection was used to

determine the purity of the sample with each detectable protein given a percent of the total detected proteins in the sample lane.

Total proteins by BCA protein assay

Total protein content was assessed using the BCA protein assay (Pierce BCA Protein assay cat # 23225, Thermo Fisher Scientific) according to manufacturer's protocol for the microplate procedure. Various sample dilutions were tested before perform the final quantification test to fall in the linear range of the assay with minimum to no matrix inhibition effect. Samples were loaded neat (20 μL/well) and in triplicates in the 96-well microtiter plate. The standard curve was prepared with BSA in WFI between 25 μg/mL and 2 mg/mL and loaded in duplicate. Upon acquiring the absorbance values at 562 nm wavelength (Synergy LX Multi-Mode Reader, BioTek Instruments Inc.), each standard and sample absorbance value was adjusted for the mean blank value and plotted against the concentration using a best fit curve (Microsoft Excel) to extrapolate the sample values. For the final sample results, five independent assays were performed and averaged. The coefficient of variability across the five assays averaged 8.51% ± 4.17%.

HCPs

The concentration of HEK293 (host cell) proteins in the final rAAV9-GFP stocks was quantified with by ELISA using HEK 293 HCP ELISA kit (Cat # F650S, Cygnus technologies, Southport, NC). The kit-provided standard was prepared according to manufacturer's instructions and loaded from 2 to 200 ng/mL in I-700 sample diluent (cat # I700-100, Cygnus technologies) in duplicate. Sample dilutions were optimized to fit within the linear range of the assay and minimize matrix interference. Samples were loaded in duplicate as neat, 2-, 4-, and 8-fold dilution in sample diluent. Matrix (DPBS) and/or sample interference was evaluated by in-test spike-in. Absorbances were acquired at 450 nm and 650 nm (Synergy LX Multi-Mode Reader, BioTek Instruments Inc.). Standard and sample absorbances were corrected by subtracting the mean value of the blank. Standard absorbances were plotted against corresponding concentrations using a polynomial best fit curve (Microsoft Excel, trendline, linear) and samples concentrations were deducted. The spike-in test showed an overall consistent 66% ± 4.06% spike recovery in samples types, including DPBS, and across the dilutions confirming that direct comparisons between samples was possible.

AAV capsid titers and percentage of full capsids by Stunner

AAV samples were assessed on Stunner using the AAV Quant application at Unchained Labs according to the manufacturer's instructions. This instrument combines DLS, SLS, and UV/Vis techniques to determine capsid titers based on.[44] In brief, the AAV Quant application measures the full UV/Vis absorbance spectrum to determine protein and ssDNA mass. The absorbance signal is converted to mass using molar extinction coefficients for each AAV sample calculated based on amino acid sequences and the expected gene insert size input into Stunner Client software. Mass is converted to equivalent titer based on input to Stunner Client software, including VP amino acid sequences, VP ratio, the proportion of post-translational modifications, and gene insert size. For this study, 2 μL of each sample were loaded in sextuplicate in a Stunner plate. The default AAV9 serotype was used in the Stunner Client software with a 3,364-bp DNA insert, with 4 DLS acquisitions of 5 s each and duplicate water blanks. Protein concentration, capsid titer, vg titers (full capsids), and percentage of full versus empty capsids were determined by Stunner.

AAV9 capsid titer by ELISA

AAV9 capsid titers were determined by ELISA (AAV9 Titration ELISA, cat # PRAAV9, PROGEN Biotechnik GmbH) according to the manufacturer's instructions. Samples were serially diluted from 1.5×10^5 to 2.05×10^7 fold. The standard curve was generated with the kit-provided standard using a second-order quadratic polynomial curve fit and sample concentrations were automatically interpolated from the standard curve (Prism). Absorbances were acquired at 450 nm (Synergy LX Multi-Mode Reader, BioTek Instruments Inc.). Concentration values were averaged across the dilutions that were within the adjusted absorbance range recommended by the vendor and the standard deviation calculated. A minimum of two and to up to three dilutions were used for each sample with a coefficient of variability of less than 5%. Owing to the high number of samples and dilutions, and based on our experience with the reproducibility of the method, replicates were not performed.

Electron microscopy

One rAAV9 sample from each production method, HSV or PEI Max, were imaged by negative staining transmission electron microscopy (TEM). Each sample (5 μL) was spotted onto carbon-coated copper 400 mesh grids (cat # CF400-CU, Electron Microscopy Sciences), blotted with dry Whatman filter paper, and followed by 3 × 10 s washes with WFI. For the staining, 10 μL of 1% uranyl acetate (cat # 22400-1, Electron Microscopy Sciences) was spotted to the dry grids for 15 s twice and blotted dry. Imaging was done on Hitachi 7600 TEM instrument in the Electron Microscopy Core, College of Medicine, University of Florida. Full and empty were manually counted using same scale picture field using ClickMaster2000 Software. Final result was obtained by averaging the count from four different field pictures for one HSV-produced rAAV9, and from 10 different pictures for one PEI-produced rAAV9.

Detection of HEK293 host cell DNA by digital droplet PCR in AAV samples

Quantification of hcDNA was performed by the Assay Development and Analytical laboratory at Resilience using the company's proprietary platform with a commonly used highly repetitive sequence within the human genome as a target for a probe-based digital droplet PCR (ddPCR) assay.

Detection of residual AAV2 Rep and AAV9 Cap DNA by quantitative real-time PCR

Packaged and unpackaged residual helper plasmid (pDG-UF9-KanR) or rHSV (rHSV-2/9) was evaluated in parallel between HSV and PEI-producer rAAV9 by quantitative real-time PCR using AAV2 Rep primer set (forward: 5′-GCAGGAGCAGAACAAAGAGA-3′ and

reverse: 5′-CACTGCTTCTCCGAGGTAATC-3′) and AAV9 Cap primer set (forward: 5′-GATGAATCCTGGACCTGCTATG-3′ and reverse: 5′-GTTGTCTCTTCCAGTTCCTTGT-3′) (see also Figure 5A). Primers were obtained from IDT DNA Corp. Purified AAV9 stocks were either treated with 10 U DNAse I as described above or mock-treated (no DNAse I) before be serially diluted over a two-fold series between 5×10^1 and 8×10^2. The PCR mix was prepared as describe above. Cycling conditions were 95°C for 10 min and 40 cycles at 95°C 10 s, 62°C 30 s (CFX Connect, Bio-Rad). The standard curve was prepared using plasmid pHSV106-RepCap9 established over a five-fold dilution series from 0.1 ng to 1.28 fg and converted in copy number.

Detection of residual HSV DNA by quantitative real-time PCR

The same procedure as described for AAV2 Rep and AAV9 Cap was followed with the exceptions that three separate primer sets were used at different location of the HSV genome: HSV UL22 primer set (forward: 5′-GGTAGGTCTTCGGGATGTAAAG-3′; reverse: 5′-CTAA ACCTGACTACGGCATCTC-3′); HSV UL24 primer set (forward: 5′-AGGTCCACTTCGCATATTAAGG-3′; reverse: 5′-AGTTTCA CGCCACCAAGAT-3′). A third set for HSV UL36 was used in combination with purified HSV DNA for the standard curve (forward: 5′-GTTGGTTATGGGGGAGTGTG-3′; reverse: 5′-TCCTTGTCTG GGGTGTCTTC-3′).

AAV replication by Hirt extracts

Expi293F cells were seeded at 1×10^6 cell/mL in 100 mL final volume and either infected with rHSV or transfection with PEI MAX (100 μg plasmid DNA, 2:1 PEI-to-DNA ratio). Cells were sampled at each given time (1.5 mL, or approximately 1.5×10^6 cells), transferred to a microcentrifuge tube, and spun down by centrifugation (5,000 rpm, 4°C, 10 min) and rinsed once with 1× DPBS. Low-molecular-weight AAV replicative forms were extracted according to the Hirt's extract protocol (ref) with some modifications. Cells were lysed in 1 mL of lysis buffer (0.6% SDS, 10 mM EDTA, 10 mM Tris, pH 7.4) for 10 min at room temperature, then incubated in 50 μg/mL proteinase K (Cat # EO0491, Thermo Fisher Scientific) for 1 h at 37°C. We added 1 M NaCl for overnight incubation at 4°C to precipitate the chromosomal DNA, which was then removed by centrifugation (30 min, 13,000 rpm, 4°C). The supernatant was carefully transferred to a new 1.5-mL tube. The low-molecular-weight DNA was precipitated with ethanol and purified using DNeasy Blood & Tissue Kit (cat # 69504, Qiagen) according to the manufacturer's instructions. Sample DNA concentration was measured by a NanoDrop spectrophotometer. AAV DNA produced by PEI transfection were digested with Dpn I (cat # FD1703, Thermo Fisher Scientific) (10 U, 37°C, 1 h). Approximately 7.5 μg of DNA was loaded on an 0.8% agarose gel and separated by electrophoresis (50 V, 6 h) in 1× TAE buffer (50× TAE, MP Biomedicals, Inc) with ethidium bromide. After separation, the DNA was transferred to a nylon membrane (neutral nylon transfer membrane, cat # 1213364, GVS) by the Southern blotting technique. Briefly, the agarose gel was incubated in a denaturing solution (AccuGENE Cat # 51227, Lonza, Thermo Fisher Scientific) for 30 min, then a neutralizing solution (cat # 51229, Lonza, Thermo Fisher Scientific) for 2 × 30 min, with two washes with distilled H_2O at every transfer. The DNA transfer was performed overnight using 20× SSC buffer (SSC buffer 20×, AccuGENE Lonza cat # 51205, Thermo Fisher Scientific). After transfer, the membrane was rinsed with 2× SSC and the DNA fixed by UV cross-linking (XL-1000 UV crosslinker, Spectronics Corporation). The membrane prehybridization was performed in 7% SDS/0.25 M sodium phosphate buffer, pH 7.2/1 mM EDTA, pH 8.0 at 65°C for approximately 2 h, followed by an overnight hybridization with an [α^{32}P] dCTP-labeled CMV enhancer/promoter probe (Random primed DNA labeling kit, Roche Diagnostics cat # 11004760001) at 65°C. The membrane was washed in 2× SSC/0.1% SDS before exposure on a phosphor screen (Amersham Biosciences) and imaged on a GE Healthcare Typhoon Trio Variable Mode Imager.

AAV Rep and Cap proteins detection by Western blot

Cells were collected from the same infection used for the replication kinetic assay described above. Approximately 4×10^6 cells (4 mL) were resuspended in 250 μL of lysis buffer and submitted to three freeze-thaw cycles. Same volume of samples was combined with 5× reducing buffer (Pierce Lane marker reducing sample buffer, cat # 39000, Thermo Fisher Scientific) from each sample, heat denatured at 95°C for 5 min, and separated on a 10% Criterion Tris-HCl Precast gels as described earlier with MW protein ladder (Precision Plus Protein WesternC, Bio-Rad). Proteins were transferred to a PVDF membrane (ImmunoBlot Low Fluorescence PVDF membrane Cat #1620264 Bio-Rad) by the standard Western blotting technique using trans-blot SD semi-dry western (Bio-Rad). After 1 h at room temperature in blocking buffer (Odyssey Blocking Buffer LI-COR # 92740000), membranes were incubated with the primary antibody: for AAV2 Rep detection, mouse mAb 303.9 anti-AAV2 Replicase (cat # AM09104PU-N, Origene) was used at 1:100 dilution, and mouse mAb HL1419 (7B) anti-Rep 68/78 at 1:25 dilution (kindly provided by Mavis Agbandje-McKenna). For AAV9 Cap proteins, anti-AAV VP1/VP2/VP3 B1 antibody was used at a 1:2,000 dilution (cat # 03-61058, ARP Inc). After overnight incubation at 4°C, membranes were washed and incubated with the goat anti-mouse infrared conjugated secondary antibody (P/N 926-32211 1:10,000) for 1 h. The blots were detected by an infrared imaging system (Odyssey LiCor).

HSV-specific assays

Plaque assay

The rHSV infectious titers were assessed by a traditional plaque assay. V27 cells were seeded at 1.2×10^5 cells per well in 24-well plates (Corning). Serial dilutions of the rHSV stocks were added to the cells and incubated for 1.5–2 h. The inoculate was removed and DMEM containing 0.8% Agar (LMT Invitrogen, Thermo Fisher Scientific) was poured in each well. Plaques were counted by microscopic examination at 72 h after infection.

Statistical analysis

GraphPad Prism software (GraphPad) was used to analyze differences between groups utilizing a one-way ANOVA followed by

Tukey's multiple comparison test. A p value of less than 0.05 was considered statistically significant.

Figures and diagrams

Figures were prepared GraphPad Prism software (GraphPad). Schematic diagrams were created using BioRender.com.

SUPPLEMENTAL INFORMATION

Supplemental information can be found online at https://doi.org/10.1016/j.omtm.2021.12.006.

ACKNOWLEDGMENTS

We would like to thank the Department of Pediatrics of UFL, and Dr. Scott A. Rivkees, for providing Departmental Seed Funds to N.C. to support this research work. We thank Dr. Chen Ling, State Key laboratory of Genetic Engineering, School of Life Sciences, Fudan University, Shanghai, China, for allowing C.Y. to join N.C. laboratory as a part of the visitor exchange program. We thank Kevin Lance from Unchained labs for his collaboration and help with acquiring the data on the Stunner. We are also grateful to Dr. Frederick A. Kweh from Resilience, Assay Development Laboratory, Alachua, Florida, for his contribution and help with conducting the hcDNA assay. We also thank Dr. Shanon Boye and her laboratory for helping with the electron microscopy technique.

AUTHOR CONTRIBUTIONS

N.C. designed the original study, performed data analysis and manuscript preparation. P.D.T, C.H.Y, P.C., and N.C, conducted small scale optimization experiments. P.D.T. and N.C. performed large-scale production batches. P.D.T. established and conducted the purifications. C.H.Y. performed AAV replication and AAV Rep and Cap gene expression experiments and analysis. P.C, P.D.T., C.H.Y, E.J., T.C., L.A., and N.C conducted analytical assays. B.J.B. reviewed the manuscript. N.K.P. helped with the study design, interpretation, and provided extensive editing of the manuscript.

DECLARATION OF INTERESTS

N.C. and B.J.B. are inventors on patent applications U1202.70016US02 and U1202.70060US00 related to this research. B.J.B. is an inventor of intellectual property owned by the Johns Hopkins University and the University of Florida related to the HSV system and has AAV patents licensed to various biopharmaceutical companies. B.J.B. is co-founder of Applied Genetic Technology Corporation, Lacerta Therapeutics, and Aavanti Bio, which may benefit from this study. All other authors declare no conflict of interest with regards to this study.

REFERENCES

1. Keeler, A.M., and Flotte, T.R. (2019). Recombinant adeno-associated virus gene therapy in light of Luxturna (and Zolgensma and Glybera): where are we, and how did we get here? Annu. Rev. Virol. *6*, 601–621. https://doi.org/10.1146/annurev-virology-092818-015530.

2. Clement, N., and Grieger, J.C. (2016). Manufacturing of recombinant adeno-associated viral vectors for clinical trials. Mol. Ther. Methods Clin. Dev. *3*, 16002. https://doi.org/10.1038/mtm.2016.2.

3. Daya, S., and Berns, K.I. (2008). Gene therapy using adeno-associated virus vectors. Clin. Microbiol. Rev. *21*, 583–593. https://doi.org/10.1128/CMR.00008-08.

4. Salganik, M., Hirsch, M.L., and Samulski, R.J. (2015). Adeno-associated virus as a mammalian DNA vector. Microbiol. Spectr. *3*, 827–849. https://doi.org/10.1128/microbiolspec.MDNA3-0052-2014.

5. Berns, K.I., and Giraud, C. (1996). Biology of adeno-associated virus. Curr. Top. Microbiol. Immunol. *218*, 1–23.

6. Li, J., Samulski, R.J., and Xiao, X. (1997). Role for highly regulated rep gene expression in adeno-associated virus vector production. J. Virol. *71*, 5236–5243.

7. Naumer, M., Sonntag, F., Schmidt, K., Nieto, K., Panke, C., Davey, N.E., Popa-Wagner, R., and Kleinschmidt, J.A. (2012). Properties of the adeno-associated virus assembly-activating protein. J. Virol. *86*, 13038–13048. https://doi.org/10.1128/JVI.01675-12.

8. Ogden, P.J., Kelsic, E.D., Sinai, S., and Church, G.M. (2019). Comprehensive AAV capsid fitness landscape reveals a viral gene and enables machine-guided design. Science *366*, 1139–1143. https://doi.org/10.1126/science.aaw2900.

9. Franzoso, F.D., Seyffert, M., Vogel, R., Yakimovich, A., de Andrade Pereira, B., Meier, A.F., Sutter, S.O., Tobler, K., Vogt, B., Greber, U.F., et al. (2017). Cell cycle-dependent expression of adeno-associated virus 2 (AAV2) rep in coinfections with herpes simplex virus 1 (HSV-1) gives rise to a mosaic of cells replicating either AAV2 or HSV-1. J. Virol. *91*, e00357-17. https://doi.org/10.1128/jvi.00357-17.

10. Goncalves, M.A. (2005). Adeno-associated virus: from defective virus to effective vector. Virol. J. *2*, 43. https://doi.org/10.1186/1743-422X-2-43.

11. Grimm, D., Kern, A., Rittner, K., and Kleinschmidt, J.A. (1998). Novel tools for production and purification of recombinant adenoassociated virus vectors. Hum. Gene Ther. *9*, 2745–2760.

12. Xiao, X., Li, J., and Samulski, R.J. (1998). Production of high-titer recombinant adeno-associated virus vectors in the absence of helper adenovirus. J. Virol. *72*, 2224–2232.

13. Clement, N., Knop, D.R., and Byrne, B.J. (2009). Large-scale adeno-associated viral vector production using a herpesvirus-based system enables manufacturing for clinical studies. Hum. Gene Ther. *20*, 796–806. https://doi.org/10.1089/hum.2009.094.

14. Kotin, R.M., and Snyder, R.O. (2017). Manufacturing clinical grade recombinant adeno-associated virus using invertebrate cell lines. Hum. Gene Ther. *28*, 350–360. https://doi.org/10.1089/hum.2017.042.

15. Lock, M., Alvira, M., Vandenberghe, L.H., Samanta, A., Toelen, J., Debyser, Z., and Wilson, J.M. (2010). Rapid, simple, and versatile manufacturing of recombinant adeno-associated viral vectors at scale. Hum. Gene Ther. *21*, 1259–1271. https://doi.org/10.1089/hum.2010.055.

16. Grieger, J.C., Soltys, S.M., and Samulski, R.J. (2016). Production of recombinant adeno-associated virus vectors using suspension HEK293 cells and continuous harvest of vector from the culture media for GMP FIX and FLT1 clinical vector. Mol. Ther. *24*, 287–297. https://doi.org/10.1038/mt.2015.187.

17. Farson, D., Harding, T.C., Tao, L., Liu, J., Powell, S., Vimal, V., Yendluri, S., Koprivnikar, K., Ho, K., Twitty, C., et al. (2004). Development and characterization of a cell line for large-scale, serum-free production of recombinant adeno-associated viral vectors. J. Gene Med. *6*, 1369–1381. https://doi.org/10.1002/jgm.622.

18. Liu, X.L., Clark, K.R., and Johnson, P.R. (1999). Production of recombinant adeno-associated virus vectors using a packaging cell line and a hybrid recombinant adenovirus. Gene Ther. *6*, 293–299. https://doi.org/10.1038/sj.gt.3300807.

19. Qiao, C., Wang, B., Zhu, X., Li, J., and Xiao, X. (2002). A novel gene expression control system and its use in stable, high-titer 293 cell-based adeno-associated virus packaging cell lines. J. Virol. *76*, 13015–13027.

20. Thomas, D.L., Wang, L., Niamke, J., Liu, J., Kang, W., Scotti, M.M., Ye, G.J., Veres, G., and Knop, D.R. (2009). Scalable recombinant adeno-associated virus production using recombinant herpes simplex virus type 1 coinfection of suspension-adapted mammalian cells. Hum. Gene Ther. *20*, 861–870. https://doi.org/10.1089/hum.2009.004.

21. Adamson-Small, L., Potter, M., Falk, D.J., Cleaver, B., Byrne, B.J., and Clement, N. (2016). A scalable method for the production of high-titer and high-quality adeno-associated type 9 vectors using the HSV platform. Mol. Ther. Methods Clin. Dev. *3*, 16031. https://doi.org/10.1038/mtm.2016.31.

22. Adamson-Small, L., Potter, M., Byrne, B.J., and Clement, N. (2017). Sodium chloride enhances recombinant adeno-associated virus production in a serum-free suspension manufacturing platform using the herpes simplex virus system. Hum. Gene Ther. Methods *28*, 1–14. https://doi.org/10.1089/hgtb.2016.151.

23. Yu, C., Trivedi, P.D., Chaudhuri, P., Bhake, R., Johnson, E.J., Caton, T., Potter, M., Byrne, B.J., and Clément, N. (2021). NaCl and KCl mediate log increase in AAV vector particles and infectious titers in a specific/timely manner with the HSV platform. Mol. Ther. Methods Clin. Dev. *21*, 1–13. https://doi.org/10.1016/j.omtm.2021.02.015.

24. Grimm, D., Kern, A., Rittner, K., and Kleinschmidt, J.A. (1998). Novel tools for production and purification of recombinant adenoassociated virus vectors. Hum. Gene Ther. *9*, 2745–2760. https://doi.org/10.1089/hum.1998.9.18-2745.

25. Hildinger, M., Baldi, L., Stettler, M., and Wurm, F.M. (2007). High-titer, serum-free production of adeno-associated virus vectors by polyethyleneimine-mediated plasmid transfection in mammalian suspension cells. Biotechnol. Lett. *29*, 1713–1721. https://doi.org/10.1007/s10529-007-9441-3.

26. Durocher, Y., Pham, P.L., St-Laurent, G., Jacob, D., Cass, B., Chahal, P., Lau, C.J., Nalbantoglu, J., and Kamen, A. (2007). Scalable serum-free production of recombinant adeno-associated virus type 2 by transfection of 293 suspension cells. J. Virol. Methods *144*, 32–40. https://doi.org/10.1016/j.jviromet.2007.03.014.

27. Park, J.Y., Lim, B.P., Lee, K., Kim, Y.G., and Jo, E.C. (2006). Scalable production of adeno-associated virus type 2 vectors via suspension transfection. Biotechnol. Bioeng. *94*, 416–430. https://doi.org/10.1002/bit.20776.

28. Rumachik, N.G., Malaker, S.A., Poweleit, N., Maynard, L.H., Adams, C.M., Leib, R.D., Cirolia, G., Thomas, D., Stamnes, S., Holt, K., et al. (2020). Methods matter: standard production platforms for recombinant AAV produce chemically and functionally distinct vectors. Mol. Ther. Methods Clin. Dev. *18*, 98–118. https://doi.org/10.1016/j.omtm.2020.05.018.

29. Hebben, M. (2018). Downstream bioprocessing of AAV vectors: industrial challenges and regulatory requirements. Cell Gene Ther. Insights *4*, 131–147. https://doi.org/10.18609/cgti.2018.016.

30. Cecchini, S., Virag, T., and Kotin, R.M. (2011). Reproducible high yields of recombinant adeno-associated virus produced using invertebrate cells in 0.02- to 200-liter cultures. Hum. Gene Ther. *22*, 1021–1030. https://doi.org/10.1089/hum.2010.250.

31. Giles, A.R., Sims, J.J., Turner, K.B., Govindasamy, L., Alvira, M.R., Lock, M., and Wilson, J.M. (2018). Deamidation of amino acids on the surface of adeno-associated virus capsids leads to charge heterogeneity and altered vector function. Mol. Ther. *26*, 2848–2862. https://doi.org/10.1016/j.ymthe.2018.09.013.

32. Rieser, R., Koch, J., Faccioli, G., Richter, K., Menzen, T., Biel, M., Winter, G., and Michalakis, S. (2021). Comparison of different liquid chromatography-based purification strategies for adeno-associated virus vectors. Pharmaceutics *13*, 748. https://doi.org/10.3390/pharmaceutics13050748.

33. Adams, B., Bak, H., and Tustian, A.D. (2020). Moving from the bench towards a large scale, industrial platform process for adeno-associated viral vector purification. Biotechnol. Bioeng. *117*, 3199–3211. https://doi.org/10.1002/bit.27472.

34. Flotte, T.R., Trapnell, B.C., Humphries, M., Carey, B., Calcedo, R., Rouhani, F., Campbell-Thompson, M., Yachnis, A.T., Sandhaus, R.A., McElvaney, N.G., et al. (2011). Phase 2 clinical trial of a recombinant adeno-associated viral vector expressing alpha1-antitrypsin: interim results. Hum. Gene Ther. *22*, 1239–1247. https://doi.org/10.1089/hum.2011.053.

35. Buclez, P.O., Dias Florencio, G., Relizani, K., Beley, C., Garcia, L., and Benchaouir, R. (2016). Rapid, scalable, and low-cost purification of recombinant adeno-associated virus produced by baculovirus expression vector system. Mol. Ther. Methods Clin. Dev. *3*, 16035. https://doi.org/10.1038/mtm.2016.35.

36. Hakim, C.H., Clément, N., Wasala, L.P., Yang, H.T., Yue, Y., Zhang, K., Kodippili, K., Adamson-Small, L., Pan, X., Schneider, J.S., et al. (2020). Micro-dystrophin AAV vectors made by transient transfection and herpesvirus system are equally potent in treating mdx mouse muscle disease. Mol. Ther. Methods Clin. Dev. *18*, 664–678. https://doi.org/10.1016/j.omtm.2020.07.004.

37. Chulay, J.D., Ye, G.J., Thomas, D.L., Knop, D.R., Benson, J.M., Hutt, J.A., Wang, G., Humphries, M., and Flotte, T.R. (2011). Preclinical evaluation of a recombinant adeno-associated virus vector expressing human alpha-1 antitrypsin made using a recombinant herpes simplex virus production method. Hum. Gene Ther. *22*, 155–165. https://doi.org/10.1089/hum.2010.118.

38. Penaud-Budloo, M., François, A., Clément, N., and Ayuso, E. (2018). Pharmacology of recombinant adeno-associated virus production. Mol. Ther. Methods Clin. Dev. *8*, 166–180. https://doi.org/10.1016/j.omtm.2018.01.002.

39. Allay, J.A., Sleep, S., Long, S., Tillman, D.M., Clark, R., Carney, G., Fagone, P., McIntosh, J.H., Nienhuis, A.W., Davidoff, A.M., et al. (2011). Good manufacturing practice production of self-complementary serotype 8 adeno-associated viral vector for a hemophilia B clinical trial. Hum. Gene Ther. *22*, 595–604. https://doi.org/10.1089/hum.2010.202.

40. Penaud-Budloo, M., Lecomte, E., Guy-Duché, A., Saleun, S., Roulet, A., Lopez-Roques, C., Tournaire, B., Cogné, B., Léger, A., Blouin, V., et al. (2017). Accurate identification and quantification of DNA species by next-generation sequencing in adeno-associated viral vectors produced in insect cells. Hum. Gene Ther. Methods *28*, 148–162. https://doi.org/10.1089/hgtb.2016.185.

41. Ye, G.J., Scotti, M.M., Liu, J., Wang, L., Knop, D.R., and Veres, G. (2011). Clearance and characterization of residual HSV DNA in recombinant adeno-associated virus produced by an HSV complementation system. Gene Ther. *18*, 135–144. https://doi.org/10.1038/gt.2010.102.

42. Rice, S.A., and Knipe, D.M. (1990). Genetic evidence for two distinct transactivation functions of the herpes simplex virus alpha protein ICP27. J. Virol. *64*, 1704–1715.

43. Clark, K.R., Voulgaropoulou, F., and Johnson, P.R. (1996). A stable cell line carrying adenovirus-inducible rep and cap genes allows for infectivity titration of adeno-associated virus vectors. Gene Ther. *3*, 1124–1132.

44. Sommer, J.M., Smith, P.H., Parthasarathy, S., Isaacs, J., Vijay, S., Kieran, J., Powell, S.K., McClelland, A., and Wright, J.F. (2003). Quantification of adeno-associated virus particles and empty capsids by optical density measurement. Mol. Ther. *7*, 122–128.